Fall 2017

An investigation of borax for sealing inflow from berea sandstone

Tri-Tris Bao Nguyen

AN INVESTIGATION OF BORAX FOR SEALING INFLOW FROM BEREA SANDSTONE

by

TRI-TRIS BAO NGUYEN

A THESIS

Presented to the Faculty of the Graduate School of the

MISSOURI UNIVERSITY OF SCIENCE AND TECHNOLOGY

In Partial Fulfillment of the Requirements for the Degree

MASTER OF SCIENCE IN PETROLEUM ENGINEERING

2017

Approved by

Shari Dunn-Norman, Advisor
Richard Brow
Mary Reidmeyer
Abdulmohsin Imqam

ABSTRACT

Well inflow control is a major challenge for the oil and gas industry. Erle Haliburton revolutionized well inflow control with his patent for cementing oil wells in 1921. Soon after, cement became the accepted material to establish well integrity and has been ever since. Cement is used in all phases of the well life cycle, and it is expected to hold indefinitely once set. Yet based on the nature of cement and the placement techniques, flow pathways may develop from improper cementing jobs or from cement degradation over time. Well integrity is especially crucial for wellbore plugging and abandonment, since the cement plugs act as barriers to flow for reservoir fluids and underground sources of drinking water. Yet large numbers of wells have 'live annuli', indicating some inflow into the annulus and the large occurrence of such wells provide motivation to explore other materials to create wellbore seals.

The following project provides a qualitative exploration of borosilicate glass for inflow control in Berea sandstone. Glass is a chemically innate material with virtually no permeability. With the ability to manipulate its chemical and mechanical properties, there is potential for glass to remedy the degradation seen in cement while forming a plug suitable for downhole conditions.

In this experiment, a sample of borax was melted on the end of a Berea sandstone sample. The project was able to form a borosilicate glass seal to the sandstone core. The permeability of the sandstone decreased by 94.57% from 95.01 mD to 5.16 mD. The glass seal had a plugging factor of 18.49. While the glass did not seal the sandstone completely, the 94.57% reduction in permeability yields promising results for future work.

ACKNOWLEDGMENTS

To my mother and father, who were among the hundreds of thousands of boat people fleeing Vietnam, who faced pillaging from pirates and imprisonment by the Vietcong, who endured hardships that I can only imagine. Thank you. To my sister, who embodies strength and courage that inspires me every day.

I am grateful to Dr. Shari Dunn-Norman for her immeasurable support and guidance. It was a pleasure working with her—the heart and soul of the Missouri S&T Petroleum Engineering Department. I want to thank my committee Dr. Richard Brow and Dr. Abdulmohsin Imqam, for their invaluable contributions; with special thanks to Dr. Mary Reidmeyer who was of paramount importance to the completion of this thesis.

Gratitude to Dr. Baojun Bai's group and Rock Mechanics for their donation of time, materials, and equipment. Thank you Jeff Heniff, Haifeng Ding and Azpuri Kaba for helping me navigate the shop and the lab.

Thank you Patti Robertson, Sharon Lauck, and Wendy Albers for helping me pass the long days in McNutt. I may never have finished without them.

Special mention to my friends from around the world. Wale, Paul, Fen, Sujay, Chen, Kiana, Shruti, Onyeka, Maria, and Will. To those who served their sentence in Rolla with me. To those long nights playing foosball in Grotto drinking street painters. To those who managed to escape Woodland. To those who found a home abroad among friends.

Do good. Impact the world. Make Sacramento Proud.

TABLE OF CONTENTS

Page

LIST OF ILLUSTRATIONS

Page

LIST OF TABLES

Page

1. INTRODUCTION

Since inception, the oil and gas industry has been challenged to control well inflows, such as maintaining overbalance during drilling, isolating different producing formations, and shutting off formation flow completely. While it was relatively easy to weigh up drilling fluids, zonal isolation and shut-off were not readily achieved until 1921. According to "Haliburton Cement Wells" (2017), Erle Halliburton demonstrated an effective means of cementing casing strings downhole. His patent for a "Method and Means for Cementing Oil Wells," helped revolutionize how an oil or gas well was completed for production, and how wells would ultimately also be abandoned (U.S. Patent No. 1369891, 1921). Figure 1.1 is a typical well construction diagram for a cased and cemented onshore well.

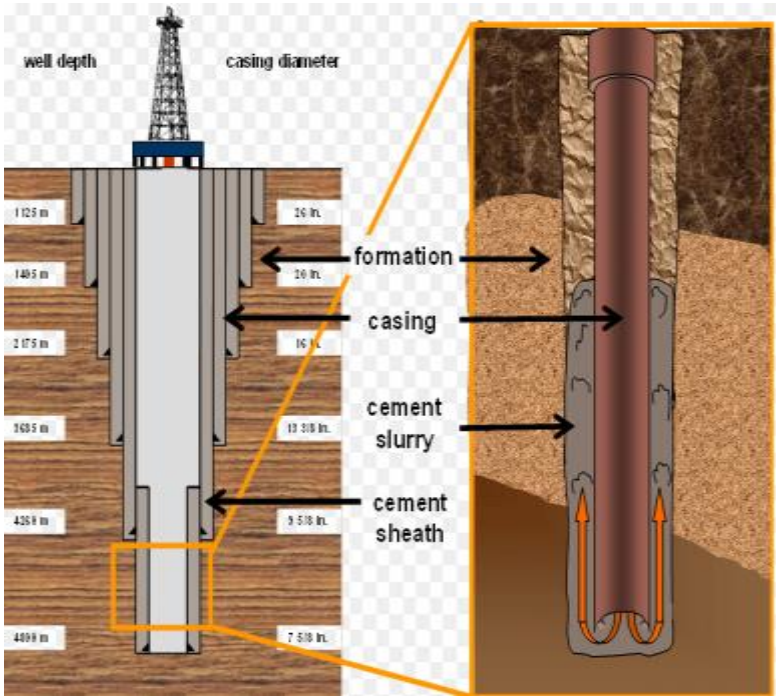

Figure 1.1 Schematic Representation of a Cemented Well. (India Cements Ltd, 2017)

Each casing string is cemented in the hole, with cement slurry either pumped back to surface, to the previous casing shoe, or to a prescribed distance above the producing formation. The cement, coupled with the casing, is expected to create wellbore integrity (a pressure and fluid seal) for the life of the well. As defined by Norsk Sokkels Konkuranseposisjon (NORSOK), the Norwegian technology center for business standard development in the oil industry, well integrity refers to the application of technical, operational and organizational solutions to reduce risk of uncontrolled release of formation fluids throughout the life cycle of a well (Standard, 2004). Cement has also been the primary material used to abandon wells when production becomes uneconomical. Typical modern well abandonment requires cement plugs across the perforated zone, across any point where a casing string is cut for removal, and at least one plug at the top of the well near the surface. Once abandoned, the cement left in the well, including the original cement behind the pipe and the cement plugs placed at abandonment, is expected to seal the wellbore indefinitely. Figure 1.2 depicts common well abandonment schematics where cement and mechanical plugs act as barriers to flow for potential flow paths. The schemes cover cases of continuous plugs in an open hole, multiple plugs in open and cased holes, and mechanical barriers coupled with cement plugs. Typically, 2-3 plugs are used in a well with one placed near the surface. If one barrier were to fail, multiple barriers help mitigate disasters by providing insurance to flow.

Despite the long history of using Portland cement within wellbores there are many limitations to using cement as a wellbore sealing agent. A brief summary of cements,

problems with oil well cementing, and industry advancements in cementing are included here as background to the current work.

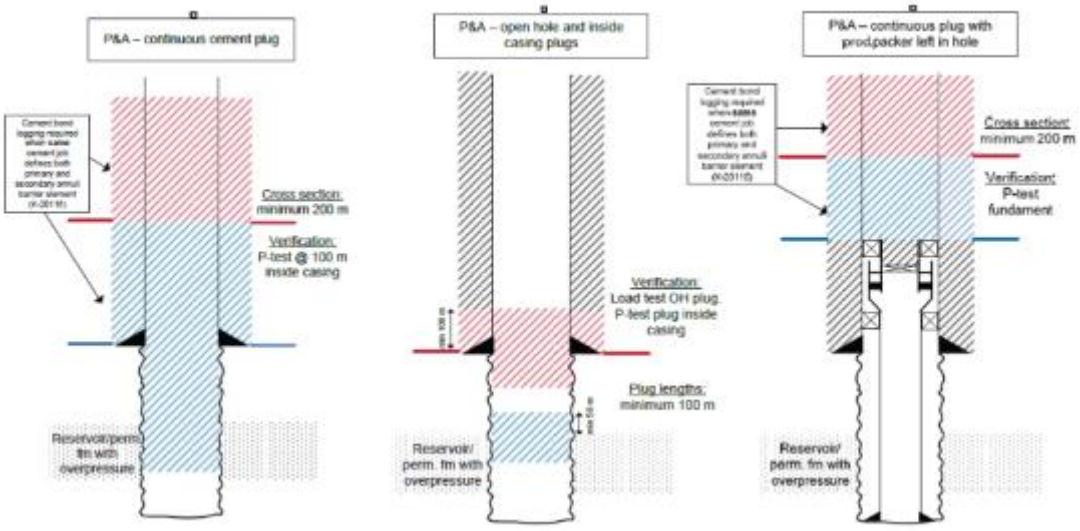

Figure 1.2 Typical Plug and Abandonment for Various Types of Well Completions (Natural Gas Investing, 2017)

1.1. PORTLAND CEMENT IN OIL AND GAS WELLS

Ordinary Portland cement (OPC) was developed by Joseph Aspdin in 1824 by burning a blend of limestone and clay together (Schlumberger, 1984). Its basic formulation remains the same, today. OPC is manufactured by crushing, milling, and proportioning the following ingredients: limestone or calcium oxide, silica, alumina, iron, and gypsum. The mix without gypsum is introduced into a rotary kiln to fuse the limestone slurry together. The kiln temperature ranges from 2,600°F to 3,000°F. Afterward, the material formed is known as cement clinker. After cooling, the clinker is

pulverized and blended with gypsum to control the setting time of the cement when water is introduced (Arnold et al., 2006).

OPC's first use in an oil well was in 1903 to shut off flow in a water zone. Eventually, the American Petroleum Institute (API) standardized the various OPC mixes that were emerging at the time for oil and gas usage. In the US, the American Society for Testing and Materials (ASTM) and API are responsible for studying and creating specifications for OPC manufacturing. Yet, ASTM is primarily responsible for construction use, while API deals with well cements. API helped identify specific industry required blends for short thickening times and late development of compressive strength (Schlumberger, 1984). These OPC blends became the accepted material for P&A for several reasons: availability, ease of placement, high strength, engineered durability, and low permeability. Table 1.1 summarizes common cement classes used in oil and gas wells. Tricalcium silicate (C_3S), dicalcium silicate (C_2S), tricalcium aluminate (C_3A), and tetracalcium alumino ferrite (C_4AF) are special compounds that help develop tailored properties for the API classes of cements.

Table 1.1 Typical Composition and Properties of API Classes of Portland Cement (Arnold et al., 2006)

	Compounds, %				
API Class	C_3S	C_2S	C_3A	C_4AF	Wagner Fineness, cm^2/g
A	53	24	8+	8	1,500 to 1,900
B	47	32	5–	12	1,500 to 1,900
C	58	16	8	8	2,000 to 2,800
G & H	50	30	5	12	1,400 to 1,700

Property	How Achieved
High early strength	By increasing the C_3S
Better retardation	By controlling C_3S and C_3A
Low heat of hydration	By limiting the C_3S and C_3A content
Resistance to sulfate attack	By limiting the C_3A content

API Classes of Portland cements are manufactured to meet chemical and physical standards for use downhole. Class A cement is intended for use when no special requirements are necessary. Class B cement is used in environments where moderate to high sulphate resistance is required. Class C cement is intended for use when conditions require high early strength. Lastly, both class G and H are intended to be used as basic oil well cement. Although these blends are standardized, additional or corrective components such as sand, siliceous loams, pozzolans, diatomaceous earth, iron pyrites, and alumina, may be necessary to optimize the cement for a specific job and create what is known as specialty cements. The additives and compositions are monitored closely. According to "Cement Composition and Classification" (2015), even minor impurities in the raw materials must be taken into account, as they can have significant effect on cement performance. For example, the additions from the coal to heat the kiln can impact the final product and its performance. According to the "Petroleum Engineering Handbook, Volume II, Drilling Engineering" (2007), these specialty cements include pozzolanic Portland cements, pozzolan/lime cements, resin or plastic cements, gypsum cements, microfine cements, expanding cements, refractory cements, latex cements, cements for permafrost environments, sorel cements, and cements for carbon dioxide (CO_2) resistance." Such cements help embellish properties such as weight, chemical resistance, and temperature thresholds.

To ensure that well cements possess the myriad of properties and characteristics necessary for downhole use, API standardized a number of tests for well cements in its publication, "Recommended Practice for Testing Well Cements" (2013). From the API publication, there are tests and apparatus for slurry preparation, slurry density,

compressive strength tests, non-destructive sonic testing, thickening time tests, static fluid loss tests, operating free fluid tests, permeability tests, rheological properties and gel strength, pressure drop and flow regime calculations for slurries in pipes and annuli, artic testing procedures, slurry-stability test, and compatibility of wellbore fluids. The wide ranges of tests help exhibit the significance and challenges of engineering cement materials and placing them downhole.

The integrity of cement is expected to extend long after the production stage. Well cement is expected to retain wellbore integrity through abandonment without degrading or losing its bond to the formation and casing. Yet, cement has a well-documented history of failure and degradation. It can fail at different times of the life cycle—well construction, completion, or later in the life—due to various operating conditions. Although oil well cement is designed to endure downhole conditions, there are substances and conditions that lead to cement failures with time. The following section will review potential conditions leading to cement failure.

1.2. CEMENT FAILURE IN WELLBORES

Achieving good cement placement when the casing is run is important during the well construction phase. A good initial cement job establishes well integrity. Afterward, cement compromise typically results from failure of the cement, cement bond, or the pipe (King and Valencia, 2014). This statement is key in analyzing cement failure as it may not be the cement itself that fails. One must also take nto account the relation between the cement with the pipe and with the formation. Figure 1.3 depicts poor cement

placements, due to the casing being eccentric in the wellbore at the time of cementing. At present, situations such as these require squeeze cementing to remediate the bond.

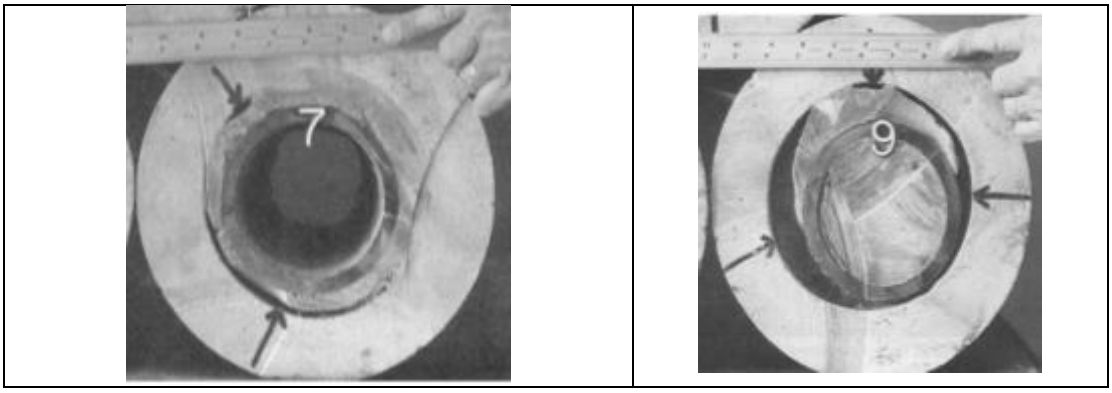

Figure 1.3 Effect of Casing Eccentricity on Cement Displacement and Bonding (Economides et al., 1998)

Figure 1.4 shows a forced gas channel was created in a laboratory setting using deviated casing (worst case scenario) (Griffith, 1992). Cementing problems such as these can often be spotted with a required mechanical integrity test (MIT), although such tests are only required periodically depending on state regulations.

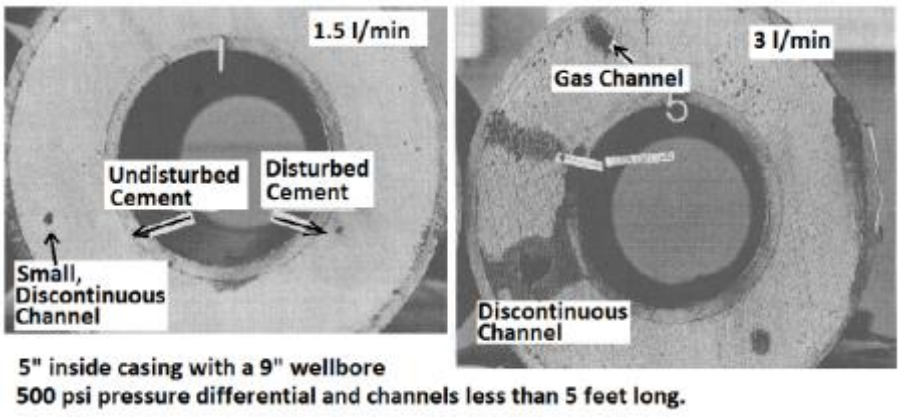

Figure 1.4 Induced Gas Channels in a Deviated, Cemented Well Casing (Griffith, 1992)

When studying the cement failures, one must ensure good initial placement of the cement slurry. Afterward, the underlying causes for fluid migration must be considered, especially over time. Issues can develop with the pipe, cement, and cement bond to the formation. Figure 1.5 summarizes the potential pathways for fluid movement in a cemented wellbore. Allowing fluids to move behind pipe can jeopardize underground sources of drinking water (USDW).

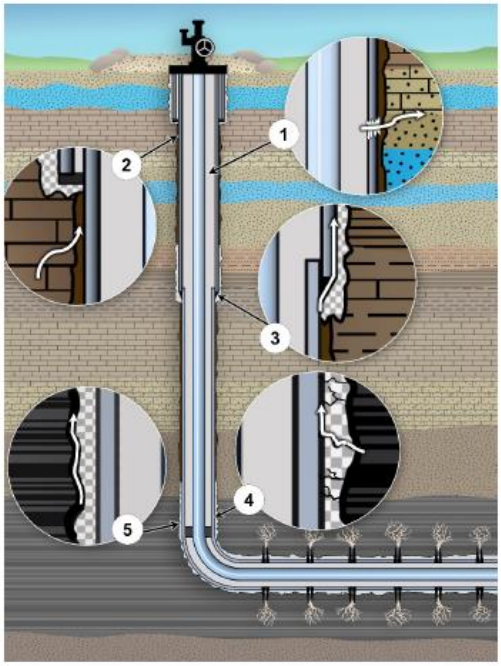

Figure 1.5 Potential Pathways for Fluid Movement in a Cement Wellbore

These pathways include: (1) casing/tubing leak into a permeable formation, (2) migration along an uncemented annulus, (3) migration along microannuli between the casing and cement, (4) migration through poor cement, or (5) migration along microannuli between the cement and formation. Note: the figure is not to scale and is

intended to provide a conceptual illustration of pathways that may develop within the well. These pathways are typically first identified by to the emergence of live annuli.

1.3. LIVE ANNULI

A live annulus refers to positive pressure detected in the annulus. Several phenomena can be grouped under the general description of a live annulus. For instance, annular pressure buildup (APB) occurs when pressure is generated from the thermal expansion of wellbore fluids. APB is a concern in well integrity as it can cause stress loading on cement sheaths and plugs that lead to failure of cement. Even with good cement placement downhole, gas may percolate into the cement before it hardens downhole, or the cement may not bond completely with the formation wall, forming a microchannel that can ultimately allow fluids to move behind the pipe. Gas percolation is also seen in scenarios of sustained casing pressure (SCP), a phenomenon where there is measureable annular pressure at the wellhead that returns after being bled down (Technologies C et al., 2012). SCP can occur early during the cementing operations or at any point in the lifetime of the well. Early signs of SCP include gas bubbling or an increase in pressure noted at the surface. SCP often occurs due to a breach in the annular seal between the casing and the formation. Unlike APB, SCP may have many causes, and is not necessarily attributed to pressure changes related to downhole temperature fluctuations.

A study analyzing the Fayetteville shale play to study issues related to SCP in hopes of determining methods of remediation and prevention (Technologies C et al., 2012). Annular surface pressure (ASP) differs from SCP in that it is an annular pressure

that has not been shown to be sustainable. In other words, ASP is a single data point at a specific time in the development of the Fayetteville shale well. Information was gathered for approximately 75 wells developed from 2006-2013. Of these 75 wells, 86.7% exhibited some sort of annular surface pressure (ASP) at some point. These wells were drilled during a 6 month period in 2013. Of these wells, 49.8% had ASP prior to hydraulic fracturing. Watters noted that 37% of wells had ASP after stimulation and that 48% of wells that exhibited ASP experienced a change (increase or decrease) in ASP magnitude after stimulation. Watters concluded that ASP occurs by two mechanisms: classic gas migration after cementing and stress induced, long term gas flow. Short term migration is seen after a few hours or days of cement slurry placement. Short term migration is controlled by pressure differential between the initial hydrostatic pressure and formation pressure, fluid loss from the cement to the formation, and volume loss during hydration. Long term migration appears weeks after slurry placement and is governed by weakness in the mechanical properties of cement, poor mud removal before the cement job, shrinkage of the set cement, damage to the cement sheath due to subsequent well operations, or some type of long term degradation method. The scope of this study did not continue monitoring pressure beyond abandonment. Yet, one must consider the long term potential for fluid migration when considering development of annular pressure with time as downhole pipes and cements age.

1.4. OBJECTIVE

The overarching objective of this project is to find a material other than cement, that could potentially seal a sandstone formation, and prove to be more durable. The

work specifically investigates the introduction of borax to a sandstone core, with the application of heat, to form a borosilicate glass, either as a coating to the sand face of the core or within the pore space of the core. Selecting the correct heating temperature, saturation method, and permeability determination are all important objectives of the project.

2. MEANS FOR CEMENT FAILURE

King and Valencia (2014) summarized that well integrity failures and plug and abandonment failures result from mechanical issues with the cement, the cement bond to the formation or piping, and the piping itself. A significant statement in the paper cites that the presence of annular pressure does not equate outright well integrity failure. Though, a live annulus may bring about concerns of well integrity. It is beneficial to study the mechanisms that drive the cause of annular pressure. These include both mechanical and chemical mechanisms. Mechanical effects include both temperature and pressure, while chemical effects cover acids, gases, salts, and bacteria. To organize the means for potential cement failure, the section will be divided into subsections that are attributed to de-bonding and methods that are attributed to cement degradation.

2.1. FLOW PATHWAY DEVELOPMENT

Over time, the system will witness various thermal cycles that will have an effect on cement sheath integrity. Reservoir temperatures are primarily governed by the geothermal gradient of the Earth's mantle. Geothermal gradients vary from 0.6°F to 1.6°F per 100 ft (Dowdle, 1975). Given the ever emerging technology to drill deeper wells, it is not uncommon to encounter reservoirs that have high pressure/high temperature conditions (HPHT) at depths of thousands of feet. As the exploration of conventional sources decline, the industry faces a growing number of HPHT wells above 10,000 psi and 300°F. During treatment and production, downhole temperatures are prone to fluctuations. Warm reservoir fluids flowing up the tubing, coupled with friction, heat up the system. Treatments, such as acidizing, inject and circulate cool fluids

downhole and lower the system's temperature. In colder drilling climates such as those found in Canada, permafrost is a major factor. Temperature fluctuations from the seasons cause the ground to freeze and thaw. With these various temperature conditions, it takes several months for the well to reach equilibrium (Bellarby, 2009). This statement also extends to well abandonment when cement slurries are placed. As the cement takes weeks to cure, it may experience temperature fluctuations during that time.

A study conducted by Andrade et al. (2015) noted the cement sheath integrity during thermal cycling. They examined debonding between cement-casing, cement-rock, and the voids and cracks within the cement after such cycling. As a result, paths develop in the annulus that provides a potential means for oil and gas flow. The sample was set at 500 psi and an ambient temperature of ~16°C. A single cycle had a thermal plate with a ramp mode of 1.5°C/min set to 130°C and held at that temperature for 4 hours. The ramp mode was then set to -1°/min for 4 hours. The ramp mode was reset to 1.5°C/min to ambient temperature. The experiment featured a cement sheath sample bound to Saltwash North sandstone and one bound to Mancos shale. Figure 2.1 shows a 3D generated computed tomography (CT) image of the Saltwash North sandstone's debonded/void volumes and cracks that were initially present, ones that formed after 1 cycle, and ones that formed after 10 cycles. The pathway development seen in the sandstone were far greater than that seen in the shale. Andrade et al. (2015) explains that this is attributed to the higher stiffness provided by the shale. The Young's modulus of the shale is considerably higher than that for the sandstone, which enhances the cement sheath resistance towards debonding and shear failures. In both samples, cement debonding to the casing was minimal. The largest contribution of fatigue came from the

initial thermal cycle rather than subsequent ones. Andrade et al. (2015) found that such integrity is difficult to maintain over time and is a cause for annular pressure and leaking issues as wells age (Kellingray, 2007 and Vignes and Aadnoy, 2008).

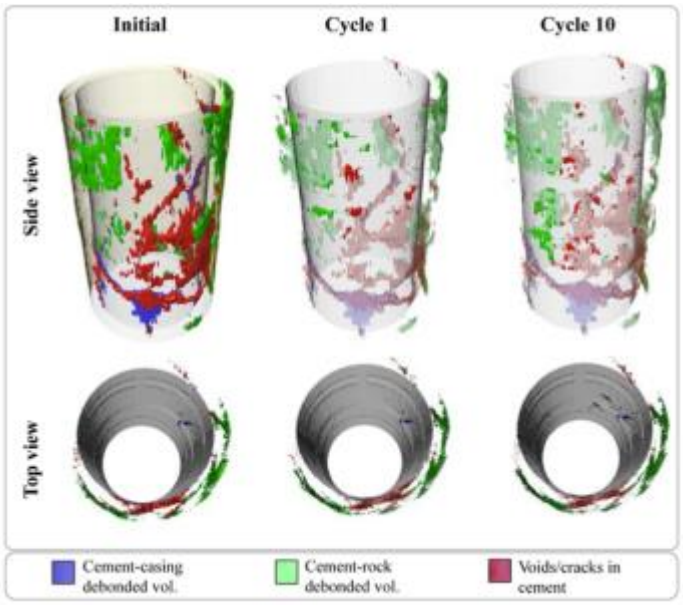

Figure 2.1 Saltwash North Sandstone Computed Tomography (CT) Sample: 3D images of debonded/void volumes, from before thermal cycles, after cycle 1, and after cycle 10. (Andrade et al., 2015)

Similar to its temperature counterpart, pressure cycles have also proven to compromise well integrity. Casing expansions caused by excessive casing pressure have shown to create radial stress cracks in the annulus (Goodwin, 1992). Goodwin (1992) cycled pressure from 0 psi to 10,000 psi in 2,000 psi increments. Between each increment, the pressure was dropped back down to 0 psi. The study conducted by Goodwin (1992) showed promising results for the ability of low compressive strength (500 psi to 1,000 psi) and ultra-high compressive strength (>12,000 psi) cement to

withstand pressure cycling. Goodwin's study found that circumferential force from excessive temperature and pressure causes diametrical and circumferential casing expansion. This expansion creates a shearing force at the cement-casing interface, causing failure at the cement-casing interface or radial fracturing of the cement sheath.

Another pressure study was conducted by Jackson and Murphey (1993). They conducted laboratory experiments to understand casing-cement-formation behavior downhole with respect to gas flow. The experiment set up both a build up and a drawdown cycle where the casing pressure was increased and held for 10 minutes and dropped down to the base pressure of 1,000 psi. The pressures tested were in 2,000 psi increments starting from 2,000 psi to 10,000 psi. For the build up test, flow was only detected during the bleed off portion for the 8,000 psi and 10,000 psi levels. Flow was not detected for the buildup portion of any of the peaks pressure levels; this included 8,000 psi and 10,000 psi that was seen for the drawdown. For the drawdown experiment, the base casing pressure of 10,000 psi was lowered in stages, to values of 8,000 psi, 6,000 psi, 4,000 psi, 2,000 psi, and below 1,000 psi. After each stage, the pressure was raised once again to the base pressure of 10,000 psi. A pressure differential across the cement was held at 100 psi. For the drawdown, little flow was noted until the casing pressure dropped below 3,000 psi. At this stage, a 100 psi differential was enough to cause flow across the 3 ft cement sheath. At pressure below 2,000 psi, a pressure differential of 10 psi was enough to cause flow across the cement sheath. At this point, the hydrostatic pressure within the inside the casing was low enough to allow flow. The initial hydraulic seal was lost when the casing pressure was dropped from 10,000 psi to 4,000 psi.

Jackson and Murphey (1996) successfully determined that it was possible to lose a hydraulic seal and when that might occur with pressure cycles.

The experiments in this section summarized laboratory recreations of downhole conditions that were successful in creating live annuli from temperature and pressure cycles.

2.2. CEMENT DEGRADATION DEVELOPMENT

Through means of chemical reaction, cement faces several degradation mechanisms. In this section, exposure to various reactants such as acids, gases, ions, and microbes will be explored to determine their role in compromising zonal isolation. This section will look at various manners that degrade cement's physical properties.

Matrix acidizing works to stimulate the well by fracturing or dissolving damage to enhance productivity. Such treatments expose perforation cement to hydrochloric acid (HCl) or hydrofluoric acid (HFl) which affect cement integrity. While playing a factor in cement degradation, P&A would primarily face conditions concerning carbon dioxide (CO_2) and sour gas (H_2S) instead.

CO_2 is a major reactant with cement for wells involving CO_2 injection. CO_2 reacts with the cement to form a layer of calcium carbonate ($CaCO_3$). According to Laudet et al. (2011), the carbonation layer progresses at a slow pace into the cement sheath at a rate of about 73 mm/year. Laudet et al. (2011) found that the carbonation front evolves linearly with time. While a reaction is noted, it has not been proven to be a driving force for loss of well integrity. Though studies are ongoing, the changes in permeability, porosity, and mechanical strength were all minimal. The reaction occurs to

such an extent that still allows for proper isolation suggesting the cement sheath can still adequately contain wellbore fluids. In regards to H_2S exposure, literature suggests the need to examine the dual interaction of CO_2 and H_2S in the system. Lecolier et al. (2006) has explored the strong impairment seen in H_2S exposure alone. Lecolier et al. (2006) found an increase in porosity and mechanical weakening of their cement. Lecolier et al. (2006) commented on the highly acidic conditions (< pH 4) of the experiment along with the time scale. Lecolier et al. (2006) believed that further studies must be conducted on a longer time scale that fit downhole conditions better to truly understand the extent of the cement change. Zeng et al. (2016) noted that a combination of CO_2 and H_2S accelerated the corrosion process, the reduction of strength and permeability wee more serious than the individual contributions from either reactant alone. Further experiments may be required to explore the relationship between CO_2 and H_2S compositions with cement over time. Yet, these studies provide an understanding of the changes in mechanical properties of cement due to these interactions.

Aside from gases, chloride degradation is a source of failure that must be considered for oil well cement. While curing in brine, the sodium (Na^+) ions are adsorbed on the calcium silica hydrate (C-S-H) surface. The adsorption decreases the Ca/Si mole ratio of the cement as Calcium (Ca^{2+}) ions are displaced and precipitated with the chloride (Cl^-) ions to form calcium chloride ($CaCl_2$). This alteration of the Ca/Si mole ratio transforms the cement properties that it was originally intended to embody.

While the seawater consists of about 3.5% salinity on average, produced water can range from 0 to 30%. A study conducted by Gowthaman et al. (2016) analyzed the effects of salinity on oil well cement. In this study, the samples were cured in different

NaCl concentrations (0-30%) with various curing periods (7-45 days). The study used uniaxial compressive strength (UCS) tests to measure the resulting Young's modulus. As a control, samples were also cured in distilled water. Figure 2.2 depicts the UCS data comparing the resulting Young's modulus over time with a given salinity level.

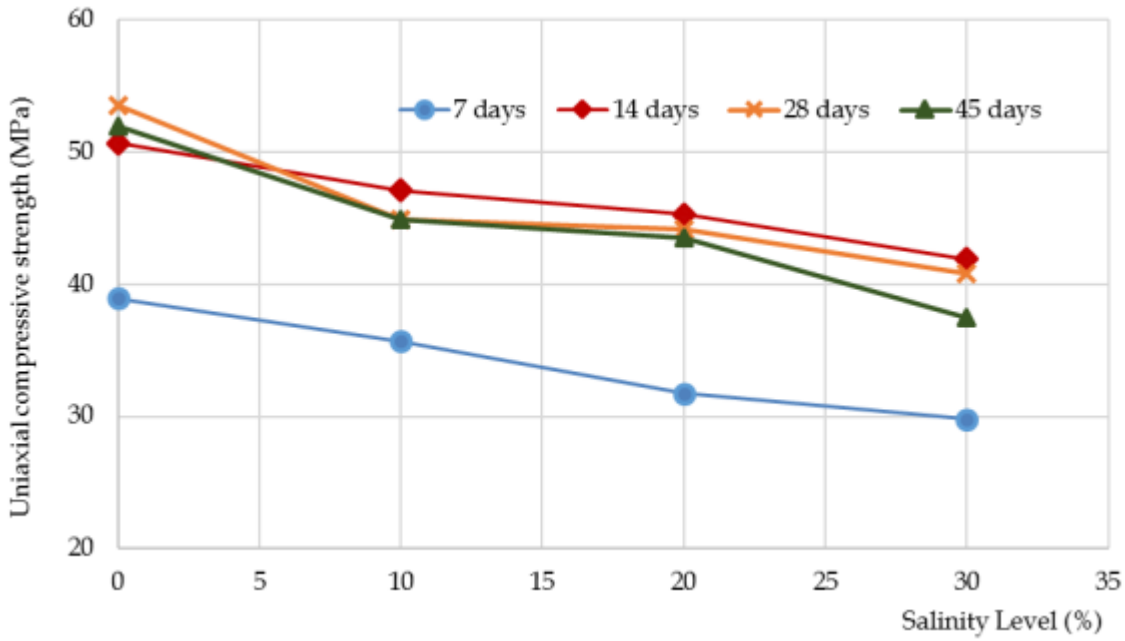

Figure 2.2 Variation of Uniaxial Compressive Strength with Salinity Level (Gowthaman et al., 2016)

Looking at the cement cured in distilled water (0%), there is an increase in UCS after 7 days of curing from 39 MPa. After 14 days, there is little change in the UCS as it hovers around ~52 MPa. Looking at the 7 day data for the other salinity levels, the UCS decreased with increased salinity levels. For 10%, 20%, and 30% salinity respectively, the UCS was about 36 MPa, 32 MPa and 30 MPa after 7 days of curing. For the trials cured in NaCl, the UCS peaked at 14 days. Moving forward for each salinity

concentration, the UCS dropped for 28 days and 45 days of curing compared to the 7 day. The magnitude of the UCS drop increased for the samples cured in higher salinity. The hydration process dominates the initial 14 days of curing, but after continued aging, the NaCl degradation becomes more notable. This paper shows the impact of brine on the cement strength, a very important consideration for the construction of injection, oil, and gas wells.

An area unexplored within the oil industry is the role of bacteria in the degradation process of cement. Known as microbiologically induced deterioration (MID), bacteria pose a threat to well integrity when considering the life of the well long after the initial P&A. Unlike chemical degradants, bacteria can exist within the cement regardless of the presence of fractures or flow pathways for fluids. The effects of MID are being studied for various structures above ground but not in wellbores or the effects on downhole cement integrity. MID stems from acid producing bacteria which exist in the environment and degrade cement components that are necessary for its structural integrity (Wei et al., 2013). Further studies may reveal MID concerns for well integrity over the long term with current OPC practices.

3. WELLBORE PLUG AND ABANDONMENT

Well plug and abandonment refers to all operations and materials used to abandon and secure a wellbore. In general, well abandonment currently focuses on placing cement plugs inside the casing string of a well, and sometimes cutting and removing some of the old casing. A more detailed examination of P&A is included here, because the experimental work performed may have the highest potential for application there.

Millions of abandoned oil and gas wells exist across the United States. These wells have received increasing attention from researchers concerned about their integrity during hydraulic fracturing (Jackson, 2014), the level of methane emissions from these wells (Kang, et al., 2016), and durability of these wells cement for CO_2 storage (Wigand et al., 2009). Many of these wells were abandoned decades ago, when abandonment standards were less rigorous. Wells abandoned in the last two decades have been subject to strict regulatory standards, overseen by each state or governing body.

Orphan wells are wells abandoned by an operator, most commonly because the operator ceases to exist prior to plugging its wells. These wells become the responsibility of the state for plugging. Like all abandoned wells, orphan wells may include older wells or newer wells. Orphan wells that are plugged by the state typically comply with modern plugging standards.

In the United States today, all wells are subject to P&A regulation at the state and/or federal level. These regulations promote healthy, safe, and sustainable practices for the oil and gas industry. Fundamentally, P&A seeks to prevent the migration of fluids in overlying permeable zones by creating barriers that eliminate flow pathways. These permeable zones contain fluids such as fresh drinking water, brine, and hydrocarbons.

Regulatory well construction practices protect groundwater and hamper the movement of unwanted fluids to the surface, bottom hole, and seafloor. Failed well integrity induces risks such as contamination of groundwater and leakage of oil and gas to the surface, sea, or atmosphere. To seal these formations, the oil and gas industry has used ordinary Portland cement throughout the last century.

Well plugging for abandonment can be divided into three different stages: preliminary activities, plugging, and plug evaluation. This section will briefly describe each stage to give an overview of the practices currently employed to abandon wells.

3.1. PRELIMINARY CEMENTING ACTIVITIES

Before cementing, two major activities are necessary for a successful P&A. First, downhole equipment must be removed from the wellbore. This can be achieved by either using existing drilling or conventional workover rigs to pull out equipment such as production tubing, downhole pumps, and packers. If such tools cannot be retrieved, alternative means must be taken on for that given situation. For example, milling is an alternative if downhole equipment becomes irretrievable.

Post-tool removal, the wellbore must be cleaned out of fill, scale, and other debris. Circulation fluid is used to catch debris and flow the material to the surface. Additional tools such as junk baskets or magnetic debris subs may be necessary to help clear the wellbore of anything the circulation fluid could not remove. Such actions are necessary to help limit contamination of the cement slurry.

3.2. PLUGGING TECHNIQUES

Cement plugging is a technique utilized in the oil and gas industry for well closure. For P&A, zonal isolation and well abandonment are the primary purposes for a cement plug (Rogers, 2006). Governing bodies require multiple plugs (both cement and mechanical) in case one were to fail in order to safeguard against fluid flow. Fields and Martin (1997) report that typically three plugs are required. The placement of these plugs includes the area around the perforation level, at mid depth (in particular over any casing cuts), and a surface plug at shallow depth. Greater or fewer plugs may be used depending on the formation, wellbore, number of fluid zones, and state regulation. Current well plugging practices use three major methods for plug placement: the balanced plug method, the dump bailer method and the two-plug method.

3.2.1. Balanced Plug Method or Displacement Method. The balanced plug method places a drill pipe or piece of tubing at the desired depth. A cement slurry is pumped through the tubular and placed on top of a mechanical device set below the point of plugging or fluid left in the bottom of the well. The mechanical device can be something such as a bridge plug, while the fluid can be mud. The slurry is pumped until the level of the cement is equal to that inside the casing. Once equal, the tubing is pulled. Figure 3.1A depicts the balance plug method. The technique is used widely due to its simplicity. Yet, concerns with this method lie in limiting contamination, especially when using a viscous plug. To prevent migration of the cement slurry, there must be a solid base material at the bottom of the well to hold the slurry in place.

3.2.2. Dump Bailer Method. According to Schlumberger (2017), a dump bailer is a tool used to place small volumes of cement in a wellbore. For the dump bailer method, the tool holds a volume of cement slurry that is run downhole and placed atop a permanent bridge plug. The bailer is opened by touching the bridge plug or opened electronically. Cement escapes the tool by raising it.Since the slurry is held stationary in the bailer, special considerations must be made for gelation and instability during the descent. The tool is easy to control and use, but it is limited by the size of the dump bailer. The balance plug and dump bailer methods are depicted in Figure 3.1B.

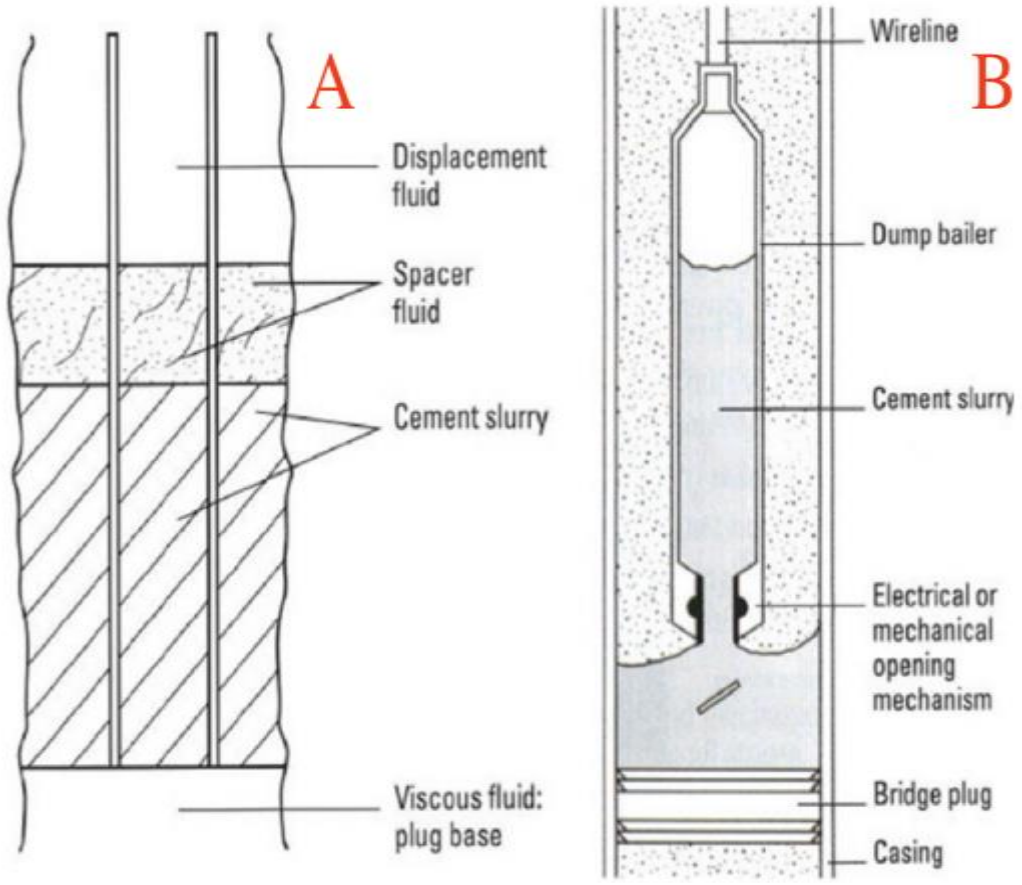

Figure 3.1 Plug Methods. A) Shows the Balance Plug Method. B) Shows the Dump Bailer Method (Global IEA, 2009)

3.2.3. Two-Plug Method. This method is the most difficult yet the most beneficial to accurately place the plug with the least amount of contamination. According to IEA Greenhouse Gas R&D Programme (2009), the two plug method uses a special plugging tool that comprises a bottom hole landing collar installed at the lower end of the drill pipe, an aluminum tail pipe, a bottom wiper plug (carrying a dart), and a top wiper plug. Figure 3.2 shows the progression of cementing plugging using the two plug method.

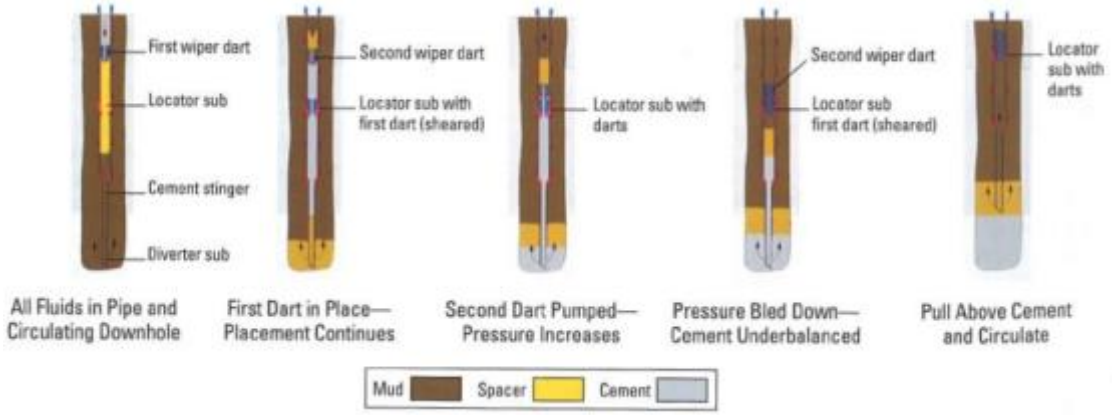

Figure 3.2 Two Plug Method (Nelson and Guillot, 2006)

The application of cementing plugs enables the effective separation of the cement slurry from other fluids, reducing contamination and maintaining predictable slurry performance. The bottom plug is launched ahead of the cement slurry to clean the drill pipe and to minimize contamination from fluids inside the casing prior to cementing. A diaphragm in the plug body ruptures by increased pump pressure to allow the cement slurry to pass through after the plug reaches the landing collar. The top plug is pumped behind the cement slurry to isolate the cement from the displacement fluid. This plug has

a solid body that provides positive indication of contact with the landing collar and bottom plug through an increase in pump pressure. The top plug then prevents cement from flowing up into the tubing string, meanwhile permitting reverse circulation. The drill pipe is pulled up until the lower end of the tail pipe reaches the calculated depth for the top of the cement plug.

3.3. PLUG EVALUATION

After the operator sets a cement plug downhole, tests must be conducted to ensure that the plug was placed at the proper depth and supports zonal isolation. The plug can be verified by tagging the top surface, pump pressure testing, or swab testing.

To tag the plug, a drill pipe, wireline, work string, or tubing is run downhole. Tagging allows an accurate measurement of the plug placement. Conversely, it applies a concentrated load at the tip of the tool place on the plug. Also, friction and buoyancy must be considered when lowering the tool for calculations. Tagging only verifies the surface depth and condition of the plug. Good results may be misleading as poor integrity below the plug surface may come with time.

The pump pressure tests consist of applying pump pressure from surface with the wellbore full of incompressible fluid. After increasing pressure, the surface gauges are monitored and must maintain pressure for a specified period of time (typically 15 to 30 minutes). This method provides accurate data for how well the plug can maintain pressure at that point in time. If the plug does not hold pressure, the operator must remediate the plug. However, after the initial testing, cement can degrade and alter plug performance.

Swabbing is another method to determine zonal isolation. A swab is run downhole to reduce pressure above the wellbore by removing fluids such that it is lower than the pressure gradient below the plug. The idea is that if the plug is holding, no additional fluids should enter the wellbore, and the swabbed fluid level should be constant. Hence, fluid levels and pressure are monitored to determine zonal isolation. Swabbing is time consuming compared to other methods but may be a preferred method in some cases.

3.4. STATISTICS OF WELL INTEGRITY AND WELL BARRIER FAILURE

It is difficult to find an exact value for well failure given the various factors involved in cement degradation, geological differences, well age, and completion design. Additionally, there is a lack of published data and follow up inspection on wells after abandonment to allow for exact failure rates. Jackson (2014) analyzes the integrity of oil and gas wells through a survey of published data to conclude values for well integrity failure. To analyze the rates, one must first define well integrity failure. Using King and King's (2013) definition, well integrity failure results in all barriers failing such that a pathway develops enabling leakage into the surrounding environment. The term 'well barrier failures' refers to individual or multiple barriers failing but not resulting in a detectable leak. Brufatto et al. (2003) analyzed 8,000 offshore wells in the Gulf of Mexico. They found that 11-12% of wells developed SCP. In comparison, Watson and Bachu (2009) reported 3.9% of 316,000 wells in Alberta had SCP. Ingraffea et al. (2014) studied 41,381 conventional and unconventional oil and gas wells drilled from 2000-2012 in the Marcellus region. Ingraffea et al. (2014) found a 1.0% well barrier failure in

conventional wells and 6.2% in unconventional wells. Ingraffea et al. (2014) also divided the wells into newer (2009-2012) and older (2000-2009) wells to determine if newer wells were any safer. According to Jackson (2014), intuitively, one would believe that older wells would have more time to develop leaks or for leaks to be detected. With better materials, stricter regulations, and greater understanding of the geologic formation with time, there is much support for this idea. Yet, Ingraffea et al. (2014) suggested otherwise. Barrier failure for unconventional wells occurred in 9.8% of wells from 2000-2008 compared to 9.1% in wells from 2009-2012 for wells found in northeast Pennsylvania. Yet, in other areas of Pennsylvania, the older wells had a failure rate of 1.5% compared to 1.9% for the younger wells. Some explanations for this difference may involve greater oversight or hydraulic fracturing in this period. In this study, the newer wells faced more inspections. Also, with increased rates of hydraulic fracturing, more failures may be caught and more failures may be likely to occur in these parts of Pennsylvania.

Given the number of wells drilled in history and the wells that must be drilled to meet oil and gas demands for the future, well integrity will remain an essential part of industry operations. With the varying rates of failure and degradation methods that act over time, statistically, it is possible for barrier failure to evolve into well integrity failure. Also, one must consider other impacts, such as hydraulic fracturing in nearby wells. The concern with multi-stage hydraulic fracturing is that the fractures created may propagate into an abandoned well with inadequate cement, and allow fluids to move upward and contaminate underground sources of drinking water (USDW). Another concern is ‘frac hits’. Frac hits describes inter-well communication where an offset well

or lateral is affected by the hydraulic fracturing of a new treatment in a nearby lateral. Frac hits are known to be violent occurrences that have been known to damage production tubing, casing, and even wellheads (Jacobs, 2007). Such damage transfers force to the cement sheaths and plugs of both parent and abandoned wells.

Well plugging is often viewed by operators as a task that provides little benefit to the company's treasury. Yet, properly plugged wells can save the company money from leakage in a field candidate for technology development. Also, it prevents cross contamination into other fields or loss of pressure for water floods or CO_2 floods which merits higher hydrocarbon recovery. The science behind P&A materials and methods has been quite stagnant. Given the initial conception of the idea and development of plugging methods and cement blends, P&A as a practice has remained relatively unchanged compared to other facets of the industry.

Based on the issues related to wellbore cementing, there is strong motivation for researchers to investigate using alternate methods of creating seals downhole. Development of new well plugging materials and methods may not only provide for more robust well construction but, depending on new technology, could cut costs over time for operators. There is no doubt that cementing technology has great room for research and development, and that any materials that improve on the current limitations of OPC would lead to significant benefits.

4. GLASS AS A PLUG MATERIAL

This project explores the potential of glass as an alternative P&A material instead of cement. Glass has been investigated and demonstrated for subsurface nuclear waste storage. Glass demonstrates excellent compressive strength and has virtually no permeability. In addition to these properties, varying composition, processing methods, and applying special finishes may introduce or alter a myriad of desired attributes. Thus, it is possible to create a glass highly suited for a given application based on thermal, chemical, and mechanical properties.

The research investigates a preliminary premise for glass as a valid material to eliminate flow in sandstone reservoirs or in combination with sand to form a wellbore plug. The project is unique in that a glass is formed in situ with the formation. In this survey, the permeability and durability of glass with the formation were prime concerns.

4.1. GLASS

Most glasses have a combination of properties not seen in other materials. Chemically durable and abrasion resistant, soda lime silicate glasses are expected to remain clear after years of exposure to the changing seasons and weather. Additionally, there is little surprise when ancient vases and containers are unearthed after thousands of year unchanged by the test of time (Phillips, 1960). With such broad capabilities, glass stands justified to be considered as a material in the oil and gas industry for its use as a plug.

4.2. GLASS PROPERTIES AND DESIGN

The most remarkable aspect of glass is the ability for its properties to be varied. In the following sections, properties that merit glass as a suitable plug will be considered. Sand is the main raw material for the most common glass, soda lime silicate. The three primary ingredients of soda-lime-silica glass are sand, soda ash, and limestone. Yet, there are other glasses that contain boron that have special properties not obtainable from the soda-lime-silica family. The principal raw materials are mixed in various combinations to form other kinds of glasses. Other materials such as fining agents, coloring or decolorizing materials, oxidizing or reducing agents, and so on may be added to create these various glasses. The final mixture of batch may be quite complex as an almost infinite variety of compositions can be produced. The fundamental steps in glass manufacturing are thoroughly mixing in the proper proportions of ingredients, melting at a high temperature, and then rapidly cooling (Phillips, 1960). This project forms borosilicate and borate glasses from a reaction of sandstone and borate.

4.2.1. Borosilicate Glass. Looking specifically at the reaction for this experiment, borosilicate glass is being formed. According to Phillips (1960) in 1915, Corning Glass Works introduced the first of a whole group of borosilicate glasses under the trademark ‘Pyrex’. These glasses revolutionized the concept of what glass can do. Borosilicate glasses have roughly three times the heat shock resistance of ordinary lime or lead glass, are usually far superior in chemical stability, and have excellent electrical properties. As a result, these glasses were used where glass was never used before at the time. Such uses included: industrial piping, centrifugal pump impellers, seals to low expansion metals, and household cooking utensils. Eventually, borosilicate glass found

its way into the laboratory as glassware. It provided an immeasurable improvement over lime glasses in all types of laboratory ware.

Like SiO_2, boron trioxide (B_2O_3) is a network glass former. Compared with soda-lime-silicate glasses, glasses that contain boron along with silica in a specific composition show an improvement in chemical and electrical properties with greatly decreased coefficient of expansion. These properties come with a moderate increase in melting temperature (Phillips, 1960). Given its high chemical durability, these borosilicate glasses prevent chemical attack and corrosion. Also, the low thermal expansivity allows the glass to withstand constant and repeat thermal cycling as demonstrated from cooking and laboratory work. These properties provide an excellent base to explore its potential as a plug for zonal isolation. Given the flexible composition of glass, these properties can be altered further to optimize its use as a plug. There are many borosilicate glass compositions other than Pyrex. A wide range of glass compositions can produce varying properties across a spectrum. Such compositions can be tailored to more desirable properties.

4.2.2. Thermal Properties. Of the thermal properties, specific heat, thermal conductivity, and coefficient of expansion, the coefficient of thermal expansion (CTE) is of major interest. Coefficient of expansion is the fractional change in length per unit change in temperature. It can be manipulated into a low value to give the glass thermal endurance, while being large enough to withstand internal stresses. For binding and sealing purposes in the wellbore, the glass's coefficient of expansion can be adapted to better match the surrounding formation. Since the project utilizes an in situ reaction, it is more likely that a composition gradient would be formed. This would yield a transition

across the materials from one coefficient to another. A smooth transition could help eliminate interfacial debonding from expansion and shrinkage due to thermal and pressure cycles.

The thermal expansion coefficient is controlled by the bond strength between the ions, the field strength of the respective ions, and the number of non-bridging oxygen atoms present. These factors are also interrelated such that altering the ratio of non-bridging oxygens would further change the bond strengths and/or the field strength present within the glass network.

For borate glasses, an anomaly occurs where the addition of alkali decreases the CTE, and then increases again when the alkali concentration reached a certain limit. The critical concentration varies from 15-30% depending on the study (Hubert and Faber, 2014). Unlike silicate glasses, the CTE increased linearly with the addition of alkalis due to the formation of non-bridging oxygens (NBO), the breaking of bridging oxygens (BO) by turning Si-O bonds and turning them into NBOs. For borate glasses, the addition of alkali contributes to the formation of four-fold coordinate boron. Increasing the alkali concentration eventually decreases the four-fold coordinated boron concentration and NBOs form on the silica-like tetrahedra. Four fold-coordinated boron bring better network connectivity within the glass and thus decrease the CTE. The higher alkali content encourages the formation of NBOs and initiate depolymerization of the network and thus increase the CTE (Hubert and Faber, 2014).

With alkalis such as Li, Na, K, Rb, and Cs, the decrease in CTE is larger for smaller ions. This phenomenon is explained by the difference in cation field strength.

Lower field strength cations tend to favor the formation of NBOs that depolymerize the network and increase CTE.

4.3. MECHANICAL PROPERTIES

The strength of glass is a topic that has been subject to great investigation. Given its wide use, it is necessary to explore its capabilities to determine safe working conditions. Yet, most of the research lacks the proper scope to identify the many variables necessary to draw a proper conclusion. Phillips (1960) compared the question "How strong is glass?" to "How fast is an automobile?". When considering the speed of the automobile, it would be appropriate to consider the type the car, age, maintenance history, kind of road, type of gasoline, and so on. Due to varying factors such as glass composition, surface imperfections (where fractures propagate), or handling, it is may be more appropriate to consider a range of possibilities for a particular case.

Theoretical estimates of the strengths of glasses are usually based on the premise controlled by the strength of silicon-oxygen bonds. Calculating the forces required to rupture these bonds in fused SiO_2 leads to theoretical strength calculations. Yet surface flaws increase stresses in the glass and decrease the strength of the material. According to Eagan and Swearengen (1978), "Additionally, phase separation, devitrification, changes in coordination number or bond strength, or changes in the susceptibility of the crack tip to environmental attack could each induce departures from the idealized relation." However, substituting B_2O_3 for SiO_2 increases the elastic modulus and strength of the glass. In addition, one can further modify the B:Na ratio to study the elastic modulus and fracture toughness. A study by Eagan and Swearengen (1978) found that

for borosilicate glasses, an optimum B:Na ratio of 0.67 had a 50% increase in strength than the best aluminosiliate glass (both containing 60% SiO_2). Though the strength of glasses is difficult to determine due to a number of factors, one can take into account special modifiers and glass composition to create tailored properties.

4.4. CHEMICAL PROPERTIES

Phillip defines chemical durability by resistance to the corroding effects of water, atmospheric agencies, and of aqueous solutions of acids, alkalis, and salts. Within the realm of materials, glass ranks highly in chemical resistance. There properties are governed by composition. Due to the possible compositions, attack by water, acids, and alkaline solutions can be prevented to provide good durability by selecting the proper glass after careful consideration. After reviewing the chemical degradants of cement, glass is capable of withstanding attack by acids, gases, and salts. The use of glass for chemical and pharmaceutical purposes demonstrates such possibilities. Yet, glasses are not always designed to be chemically durable. For example, biomedical use of glasses sometimes requires a soluble glass that dissolves in certain conditions or after a given time period.

Comparing the Na_2O-$2B_2O_3$ glass to the Na_2O-B_2O_3-SiO_2 glass, the addition of Si-O bonds that help inhibit hydrolysis from water in the glass. Thus, the borate network only glass is more susceptible to hydrolysis and more soluble in water. A composition higher in Si-O bonds would help decrease the solubility in water. Although the silicate improves the durability Bunker (1994) found that silicate glasses with boron have the highest durability when a certain ratio of B:Na. According to Bunker (1994), “The role

of network structure and chemistry in borosilicate leaching can be illustrated by considering glasses having a fixed silica content and systematically varying the Na_20/B_2O_3 content. In sodium-rich glasses, most Na^+ is associated with non-bridging oxygens, and the dissolution of the glass mirrors that of simple sodium silicate glass. As Na_2O decreases and B_2O_3 increases, all boron initially enters the silicate network as tetrahedral borate groups, decreasing the mole fraction of sodium associated with non-bridging oxygens and decreasing dissolution rates."

5. LITERATURE REVIEW

An extensive literature review was conducted related to creating glass linings in the wellbore, prior to adopting the experimental work described in this thesis. After undertaking the experimental work, the nuclear waste literature was consulted. Hence the literature review is categorized into two main topics, waste storage and rock melting, and provides examples studies in these areas. There is an additional section on currently developing technology for drilling that covers work with relevant knowledge without direct application. Waste storage explores the realm of glasses and their role in storing wastes for nuclear, oil, and gas. The topic of rock melting has been explored to reinforce boreholes in place of casing. The glassy material left behind from rock melting helps answer questions and suggest further research into the area of glass as a plug. The developing drilling technology section covers work involving laser and plasma drilling. Although the application of the work is different, there are pieces of knowledge that may be useful for this project.

5.1. GLASS FOR WELLBORE WASTE STORAGE

Lowry et al. (2015), explores the idea of utilizing thermite, a material that gives off a highly exothermic reaction when ignited, to form an in-situ self-sintered ceramic plug from the surrounding formation. Although the original publication targeted boreholes for nuclear waste disposal, the project has evolved for application within oil and gas, geothermal, CO_2, and nuclear boreholes. For the initial nuclear application, Lowry et al. (2015) sought to find a plug that could be placed at depths of up to 16,000 ft. The plug must perform under high hydrostatic and lithostatic pressures in high mineral

content water, and at elevated temperatures due to the geothermal gradient. The conventional nuclear plug methods rely on hydrated cements used in the oil industry. Yet, there is an emphasis placed on the performance requirement for nuclear waste disposal on the scale of thousands of years. With controlled studies, Lowry et al. (2015) was able to create plugs with compressive strengths as high as 100 MPa (about three times the strength of well cement) and fluid permeability as low as 100 μD. The plugs possessed the corrosion durability and service temperatures of ceramic matrices. With adjustments to the basic formula, additives can modify the final material so that is exhibits attractive structural, sealing, and corrosion properties. The strength was achieved within 1 day of forming the ceramic, which outpaces the current setting time of cement.

Another interesting area of research lies in glass vitrification. There are many publications on the topic of vitrification of nuclear waste. Ojovan et al. (2007) provides an excellent overview and introduction to the idea of vitrification. Vitrification is the transformation of a substance into glass. In the nuclear waste fixing, transforming nuclear waste into a highly durable and chemically inert state. Ojovan et al. (2007) explores vitification into borosilicate glass for its chemical durability or leaching resistance.

Vitrifications studies show borosilicate glass proves to be an attractive material for its chemical durability. Due to the long half-life of nuclear waste, viritifcation addresses the potential for the introduction of radioactivity into the biosphere via water by controlling the leach rates. Such explorations help further support the use of borosilicate glass as a plug for oil and gas usage.

Manaktala (1992) conducts a thorough assessment of borosilicate glass as a high level waste form. When manufacturing waste glasses, there are several considerations that can carry over for the scope of this project. There is often a compromise between chemical durability, ease of manufacturing, and economic considerations. Sodium and lithium have strong influence on the viscosity of the melt. Depending on the molar ratio, the use of sodium and lithium together can be more effective than their individual contributions alone. In addition, Al, Ca, Mg, Zn, and Ti are also added in the form of oxides to adjust viscosity. The overall formulation comprises of glass formers, modifiers, and intermediates with the high-level waste (HLW) oxides. According to Manaktala (1992), "the structural framework of the glass is provided by the SiO_4 tetrahedra. The silicate tetrahedra were bonded together by sharing ionic-covalent bridging oxygen bonds. Other multivalent species, such as B^{3+}, Fe^{2+}, Fe^{3+}, rare earths, and actinides were also bonded within the network by bridging oxygen bonds. Low valence ions such as Na^{+}, Cs^{+}, Sr^{2+}, etc. were bonded into the network by sharing various nonbridging oxygen bonds depending upon the size of the ion." These additives can be useful for the purposes of this research project in how they can affect the glass properties.

5.2. ROCK MELTING IN WELLBORES

One of most extensive rock melting research projects, the Subterrene program, was conducted by the United States government in the 1970s. Goff et al. (1994) reviews and summarizes this research. The premise of the project was to electrically heat a graphite or molybdenum penetrator to melt a hole as it pushed through rock. As the molten material cooled, it consolidated into a glass lining. Figure 5.1 depicts the

penetrator to create the glass lining. This glass lining reinforces the borehole to prevent collapse and to minimize crossflow and lost circulation.

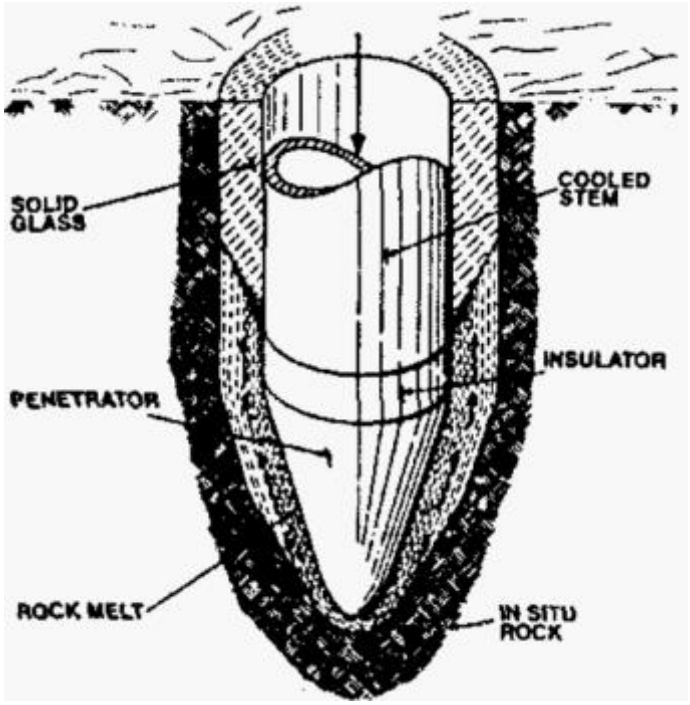

Figure 5.1 Schematic Representation of the Penetrator (Goff, 1994)

The motivation behind this research was to revolutionize how geothermal wells were created. This project was meant to serve as a proof of concept experiment and demonstrate that a rock melting tool was capable of forming boreholes in a variety of rock types. Also, it was meant to demonstrate the feasibility and competiveness the method in relation to common mechanical drilling techniques.

The program was able to create over 20 vertical and horizontal holes ranging from 2.5 cm to 10 cm in diameter and up to 30 m in length. The rock types ranged from granites, basalts, tuffs, to unconsolidated sands and soils. However, the rate of

penetration was 1 m/hr. This rate was not enough to compete with conventional methods which averaged 3 m/hr to 6 m/hr. The rock melt consolidated in situ into an impermeable, potentially strong glass lining that could alleviate hole collapse and isolate the well from permeable zones. Such work has potential for niche areas where cementing or casing operations are expensive with conventional drilling. For the purpose of this project, the Subterrene program is a proof of concept for the potential of glass as a means for zonal isolation. The project spoke about modifications to rock melting drilling to introduce reagents and thinners into the melt to increase rate of penetration and glass liner properties.

The Subterrene project published a great deal of information about its potential usage and the preliminary work done as a proof of concept. Yet after the program was halted, no further research was conducted or published. Li et al. (2015) published a paper with a similar idea to the Subterrene program. Although the research presented by Li et al. (2015) provides a clouded and odd study to mending a borehole wall, its value lies in the creation of a sheath of glassy material through insertion of a heating element into a rock sample. The element relied on heating at a conical tip to melt the rock into a molten material. Cooling of this molten rock leaves behind a glassy sheath that is integral to the rock along the element's path of travel. Figure 5.2 shows the results from granite and soil penetration. Outside of the proof of concept, the paper does not provide much more for the scope of knowledge. One aspect that is not described in detail is the formation of this glass sheath from rock formulations created by the researchers. The individuals sought to create a shale-like composition.

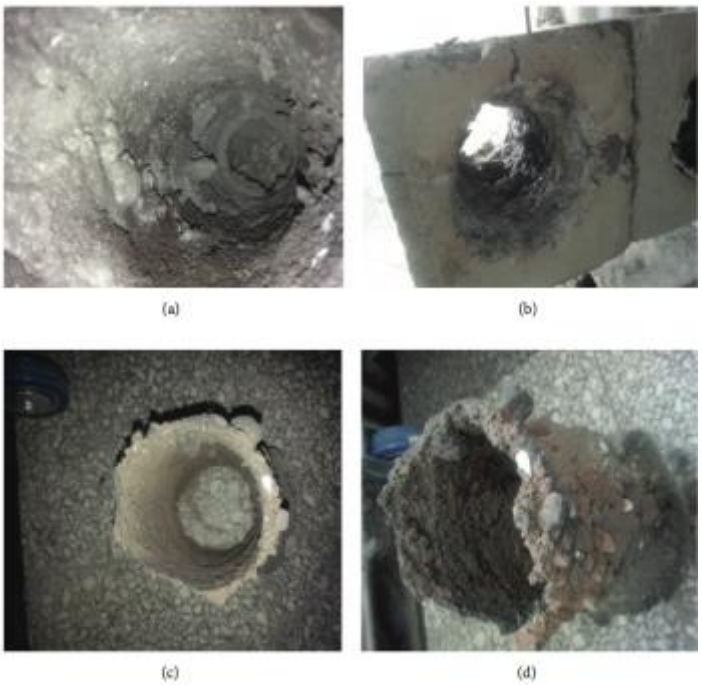

Figure 5.2 Experimental Glass-like casing: A) Top view of granite penetrated at 700°C. B) Angled view of granite penetrated at 700°C. C) Top view of soil penetrated at 700°C. D) Side view of soil penetrated at 700°C (Li et al., 2015)

Li et al. (2015) tested various compositions of raw material (RM), aluminum, and quartz. RM was provided by a manufacturer known as Zhuhai Xuanyang Limited, but the components of the raw material were otherwise not described further. Yet, the experiments proved the idea of drilling and support for even shale formations. This idea opens up the possibility for glass bonding to a formation in both conventional and unconventional formations. Given the experiments with granite and soil, it proved possible to penetrate through several different types of formations as well to form a lining.

5.3. ALTERNATIVE DEVELOPING DRILLING METHODS

It should be noted that there is a body of literature related to lasers and electric plasma. Although this technology may provide insight as to how glass forms with in situ melting in a wellbore, the literature focuses on drilling related aspects of the work. Other publications describe the use of plasma torches downhole for hydraulic fracturing and the abandonment efficiency improvement for casing removal during P&A.

Graves et al. (2002) conducted a study on the effects of reservoir rock strength and mechanical properties after undergoing temperatures induced by high power lasers. Graves et al. (2002) used the chemical oxygen-iodine laser (COIL) developed by the US Airforce. The study used 5 rocks: two Berea sandstones and three reservoir samples; Ratcliff limestone, Mesaverde shaly sandstone, and a Frontier shale. The rocks properties were measured before the experiment. Using thin section with a point-count technique, the mineral percentage was determined for each rock. X-ray diffraction (XRD) was then conducted to confirm mineralogy results. Scanning electron microscopy (SEM) was used to quantify the thermal effects of the laser. Porosity, permeability, thermal conductivity, and strength analysis were also conducted before the laser treatment for comparison purposes.

The experiment found that the thermal conductivity, the quantity of heat transmitted through a unit volume in a unit time, was significant. A higher thermal conductivity will lead to a wider range of temperature distribution and therefore greater changes as demonstrated by the behavior of sandstone and limestone. Also mineralogy plays an important role to rock changes during lasing. Micro-fractures tend to develop in quartz, clays will dehydrate, and limestones will disassociate at temperatures of 1,100°C

or greater. At 573°C, quartz grains will expand by 0.45% of their original size and contract upon cooling (Fraser, 2005). For a sample with low void space, the expansion causes full grain contact and a situation where the grains have no place to expand. This will result in micro-fractures, which also increases the void space. Micro-cracks also form during cooling of the grains. This was proven by the high quartz content sandstone that had microfractures after lasing while the limestone, with no quartz, had none. Although not discussed in the Graves et al. (2002), the limestone should have dissociated and loss strength after lasing. The Mesaverde shaly sandstone with the least void space had the greatest change in properties due to the formation of cracks in the thin section when it previously had none. Also, dehydration of clays results in an increase in the void space of rocks. Smectite clay collapses and dehydrates at 550°C. From the samples analyzed, Frontier shale has the largest clay percentage, and it also saw the largest increase in porosity. Thus mineralogy plays an important role in fracture formation. Clays contain chemically bonded hydroxyls and at high temperatures when dissociated, the water vapor escapes. This increases the volume and pressure in the pore and can cause fractures. These changes in void space may or may not change permeability, but they will ultimately affect calculated porosity and elastic moduli.

To summarize the work of Graves et al. (2002), the lasers increase porosity and permeability. The increase was more significant for high thermal conductivity sandstones but less with low thermal conductivity limestone. The strength of the rocks was reduced in all the rock samples due to the formation of fractures. The porosity and permeability changes were summarized into two categories: development of macro- and micro-fractures and the temperature effects on mineralogy (dehydration or expansion of

minerals). Near the hole, the sandstone and limestone showed an increase in permeability. Yet, the low thermal conductivity limestone showed no change away from the hole due to the lack of heat transfer. Also since clays contain water, subjecting them to high temperature will induce the escape of vapor that increases the volume and pressure in the pores to cause fractures.

These results will be significant for future studies. Although a laser was the heat source for this sample, the changes in reservoir rock strength and mechanical properties must be taken into consideration for well integrity. Other heat sources would cause similar effects in the near wellbore region due to thermal conductivity. Since the formation-plug bond is a potential area for failure, the ability to manipulate such effects can be beneficial for zonal isolation work.

As of late, a great body of work exists for the potential of plasma torches in the oil industry. The focus lies in its use for hydraulic fracturing (Bazargan et al., 2014), drilling, and milling (Kocis et al., 2015). Based on the thermal conductivity effect to cause fractures and increase void space as previously discussed (Graves et al., 2002), Bazargan et al. (2014) takes advantage of this effect by forming macro- and micro-fractures in rock samples. The Bazargan et al. (2014) experiment looks to model and simulate such effects in hopes of utilizing it to facilitate hydraulic fracturing in the wellbore. For zonal isolation, these results are unwanted due to the increased conductivity of the reservoir. The work by Kocis et al. (2015) takes the technology in another direction with drilling and milling. In comparison to hard rock (conventional rotary) drilling, the plasma technology relies on thermal characteristics of the rock (boiling point, melting point, and thermal conductivity) to determine rate of penetration

(ROP) instead of mechanical properties as seen in hard rock drilling. The modes of disintegration possible are distinguished by plasma temperature: spallation, melting, and evaporation. Looking at the melting portion of disintegration, Kocis et al. (2015) analyzes spin-off technology. Well stability enhancement is briefly mentioned as a plasma tool creates a vitrified layer in the wellbore which may serve as a 'temporary casing' since its mechanical properties are insufficient for long-term use. The researchers mention the possibility of in-situ casing creation from additive layering of metal powder on the walls of the well to enhance stability. They also bring up its potential for borehole repair of existing wells.

Looking at body of work available for these mentioned alternative drilling methods, the thermal effect of high temperatures on rock must be taken in account. In terms of well integrity for this project, it brings about valuable results such as a vitrified layer in the wellbore. Yet, it is a double-edged tool in that the potential for fracture formation, mechanical weakening of the formation, increased permeability, and increased porosity call for careful planning and research to properly conduct research.

6. PROJECT DESCRIPTION

This project explores the possibility of borosilicate glass as a wellbore sealing material in Berea sandstone cores. The project reacts borax ($Na_2B_4O_7 \cdot 10H_2O$) directly with sandstone (SiO_2) cores by melting a borax pellet on the end of a core saturated with borax. An investigation of the best melting temperature was conducted on smaller sandstone discs to determine the core reaction temperature.

The experiments include core flooding to determine if a change in permeability occurs. The permeability of the unreacted core was compared to that of the reacted core, to quantify any changes in permeability as a result of the glass formation in the core. This section details the experimental work conducted in the research.

7. EXPERIMENTAL SETUP

The following section provides a description of the setup and equipment used in the research. The equipment used included a Thermolyne 1200ºC Muffle furnace, a Denver Fire Clay dish to hold Almatis tabular alumina (14-28 mesh), the Berea core, and borax (Sodium Tetraborate Decahydrate Fisher Sci S246-212, 99% purity) pellet (Figure 7.1), a diamond blade (for cutting), a container for boiling and saturating the core, and a permeability core flooding apparatus.

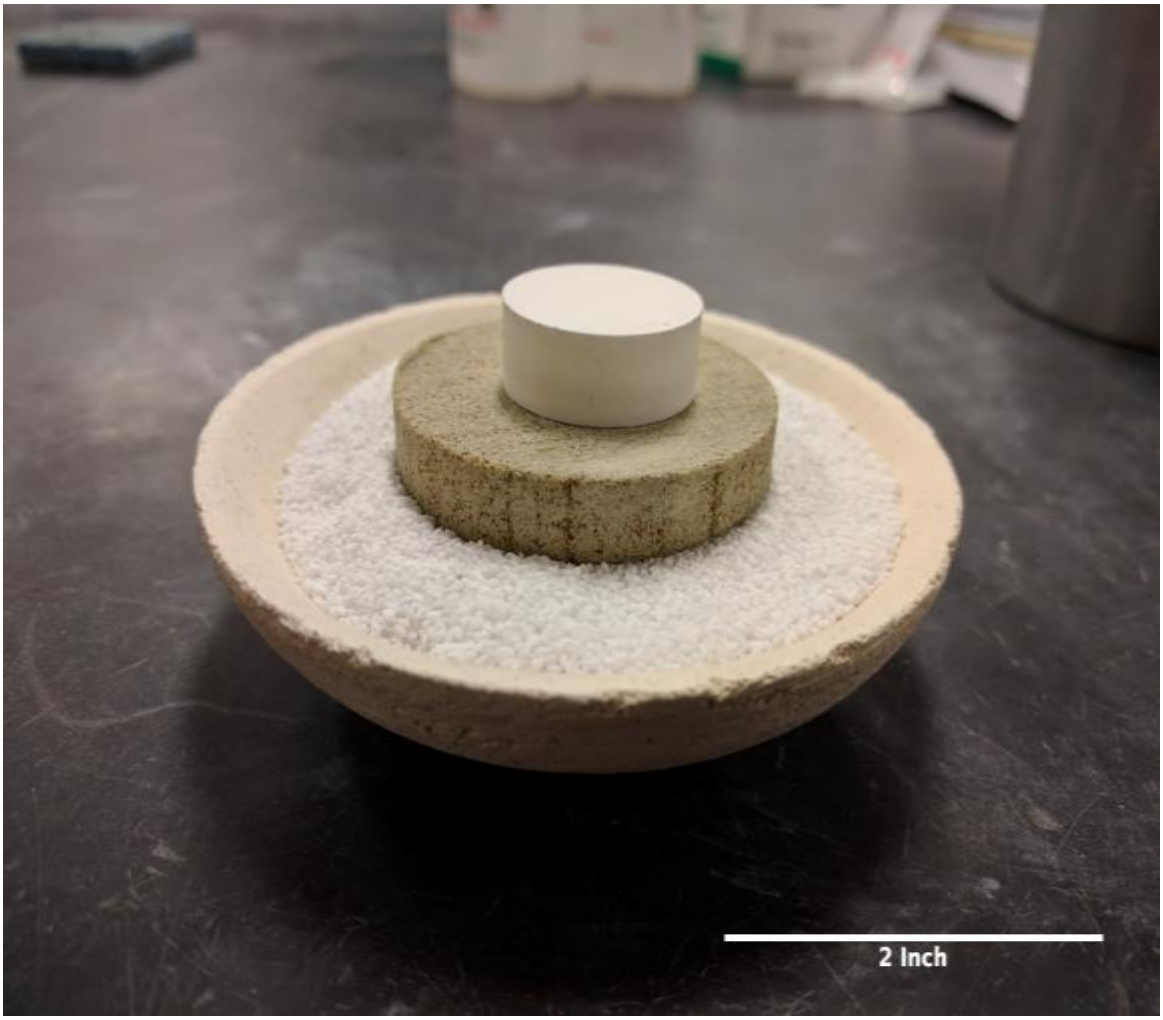

Figure 7.1 Sandstone with the Borax Pellet Ready for the Furnace

7.1. PERMEABILITY MEASUREMENT APPARATUS

The core flooding apparatus used in this work is shown in Figure 7.2. The apparatus consists of a fluid container, syringe pump, pressure gauges, and a 2" core holder. Fluid travels from a container through a pump where it was then flooded through a core. The core was held in place by a core sleeve which provides confining pressure from a radial force. The pump was set to flow at a constant rate for the fluid inlet. A gauge was set at the core sleeve inlet to measure the fluid entry pressure. The confining pressure was set above the entry pressure to ensure that flow occurs through the core sample and not around it. Since the outlet was unconfined, there was no need to measure the atmospheric outlet pressure.

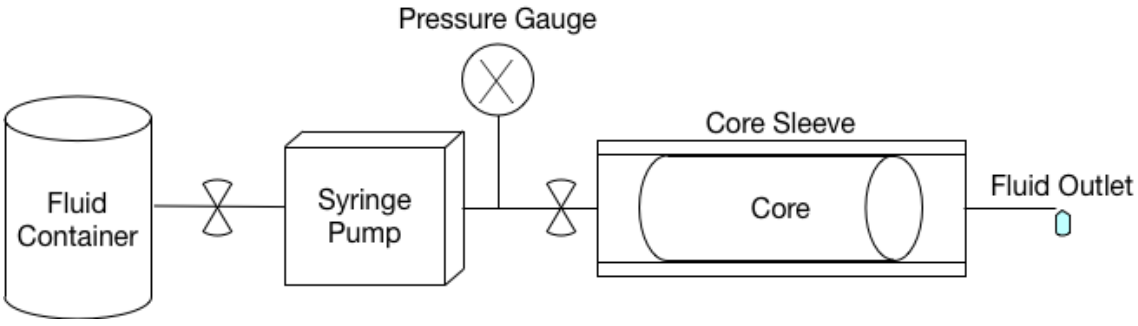

Figure 7.2 Core Flooding Apparatus

The core flooding measurement was based on the linear form of Darcy law (Equation 1). In Equation 1, the variables q, k, A, P, μ, and L respectively, are flow rate (ml/min), permeability (mD), cross-sectional area (cm^2), pressure (psi), viscosity (cp), and length (cm).

$$q = \frac{kA\Delta P}{\mu L} \qquad (1)$$

$$k = \frac{q\mu L}{A\Delta P} \qquad (2)$$

By rearranging Equation 1, Equation 2 gives a direct relationship to determine the permeability from the flow rate, fluid viscosity, pressure differential across the core, cross sectional area, and length of the medium. All factors of Equation 2 were known, except entry pressure which must be measured experimentally to determine permeability. The exit pressure was atmospheric, so the value of ΔP was equal to that of the fluid entry pressure.

Darcy law was used to measure the permeability of the sandstone core. To use the Darcy equation, one of the assumptions is that the porous medium is 100% saturated with a given fluid. To saturate the sample, the core was placed in vacuum chamber to remove the air from the pore spaces. A 1% solution of brine (NaCl) was drawn into the chamber while under a pump to maintain the vacuum pressure and displace any residual air. The incoming brine fills the pore spaces to satisfy the assumption for Darcy law of 100% saturation.

7.2. SATURATING CORES WITH BORAX

To introduce borax into the sandstone pores, the sample was boiled in a 27 wt. % solution of borax. By gas expansion through heating, air escaped the pores. The gases occupying the pore spaces were then displaced by the borax solution. Boiling occurred

over the span of 5 hours to ensure proper penetration and saturation. After boiling, the sandstone core was dried in an oven at 110ºC to vaporize the water. The process worked to deliver borax into the pore spaces and produce a dry sandstone sample. When the water was vaporized, the solute (borax) remained in the voids of the Berea sandstone core.

8. EXPERIMENTAL PROCEDURES

A Berea sandstone core was used for the research project. The sample was first analyzed using XRD to determine mineralogy. The permeability of the unreacted sandstone core was measured according to the procedures outlined in Section 7.1. After measuring the unreacted core permeability, a series of melting experiments were conducted to determine how the melted borax covered the end of the core and the nature of the glass product formed. Thin sandstone discs were cut. These discs were placed into a furnace with a pressed (made from ~500 lb-f) borax pellet on top as seen in Figure 7.1. Looking at Figure 8.1, the ternary diagram describes the potential products of the reaction. Na_2O-$2B_2O_3$ (the phase produced when borax is dehydrated) has a melting temperature of about 743ºC. Looking at the isotherm lines, there is a decrease in temperature moving inward (following the red arrow) on the diagram. The heavy curving lines that cross this region are liquidus lines. The lines move downward in temperature and there are intersections of these lines—peritectic then eutectic points. The lowest temperature where some liquid can be formed is the eutectic, which is something below 600ºC in this reaction. Here, the reaction can potentially begin to form liquid in some localized area of the specimen despite being below the melting point of Na_2O-$2B_2O_3$, 743ºC. Since the phase diagram is in equilibrium, it was unknown how long it the kinetics require to reach that point. Thus, the reaction becomes a kinetics versus equilibrium problem. The melting experiments were conducted below the melting point of Na_2O-$2B_2O_3$ starting at 700ºC. Each program gradually brought up the temperature and examined in case the kinetics were fast enough to obtain a melt at lower temperatures.

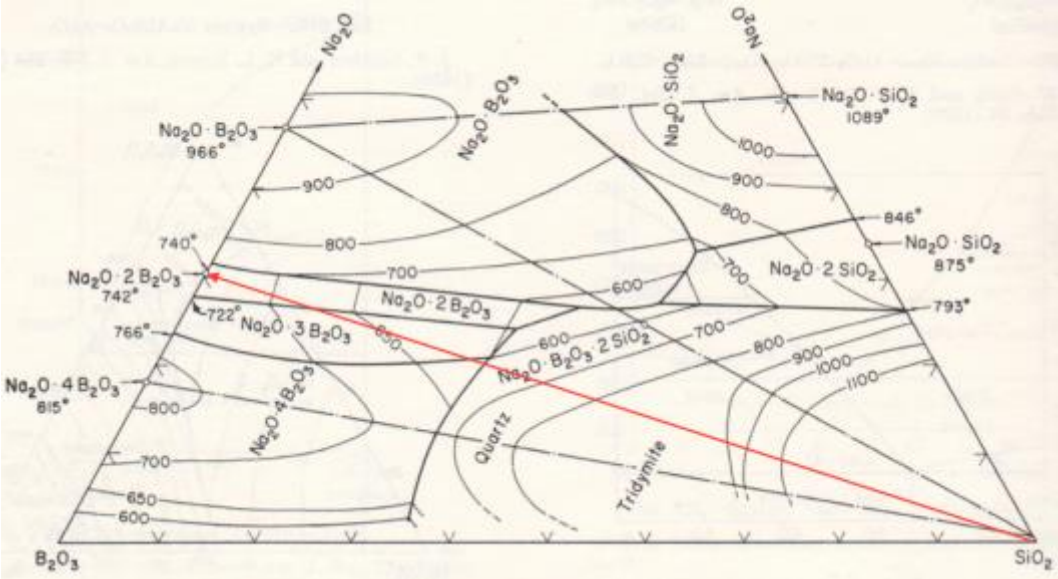

Figure 8.1 System Na_2O-B_2O_3-SiO_2 (Morey, 1951)

The sandstone discs were reacted at various temperatures to help identify the best peak temperature and hold time, to form a glass on the end of the core. After cooling the discs, the samples were cut in half to evaluate the depth of penetration of the borax-sandstone reaction. The reaction formed a glass layer that sat atop the sand face and glass that penetrated into the pore spaces below the sand face. To remove any dehydrated and unreacted material, the samples were soaked in deionized water. Comparing the Na_2O-$2B_2O_3$ glass to the Na_2O-B_2O_3-SiO_2 glass, the addition of Si-O bonds help inhibit hydrolysis from water in the glass. Thus, the borate glass is more susceptible to hydrolysis and more soluble in water. A composition higher in Si-O bonds characteristic of all silicate glasses would help address the solubility in water.

After determining a proper reaction temperature, the goal of the project was to form glass inside of the reacted sandstone core in addition to forming a glass seal at the

end of the core. Afterward, the permeability of the reacted core was measured to see how the seal may have reduced permeability and prevented flow.

8.1. X-RAY DIFFRACTION (XRD)

The Berea sandstone's mineralogy and clay content were analyzed using a PANalytical X'Pert Multipurpose Diffractometer with a Cu x-ray source. Phase analysis was performed utilizing PANalytical X'Pert HighScore software, version 2.2e.

8.2. UNREACTED CORE PERMEABILITY MEASUREMENT

To measure the permeability of the unreacted core, the sample was first placed in an oven at 110°C for 24 hr to vaporize any liquid in the pores. The sample was then weighed to find the dry weight and brine-saturated weight using the procedures listed in Section 7.1. The core sample was placed under a pump vacuum for 6 hours before a 1% brine solution was introduced into the chamber. The sample then remained pressurized at 12 psi for an additional 12 hr. The sample was removed from the chamber (assumed to be 100% saturated with brine) and weighed once again to obtain a brine saturated weight. The difference between the brine saturated weight and the dry core weight denotes the fluid volume or mass within the sample. This volume was used to determine the pore volume and interconnected porosity by also using the core's bulk volume.

After brine saturation, the sample was placed into the core sleeve with a confining pressure of 500 psi. A 1% brine solution was pumped through the core at flow rates from 6 ml/min to 2 ml/min. The entry pressure was measured and recorded until a stable value

was given for the respective flow rate. The stable entry pressure was recorded for each flow rate and used to determine respective permeability values from Darcy law.

8.3. REACTION TEMPERATURE DETERMINATION

To determine a suitable reaction temperature, preliminary tests were done to study the durability of the glass formed. Sandstone approximately 2 inches in diameter and 0.5 inches in thickness were cut and placed into a furnace. Individual 1" diameter borax pellets around 4.5 g were pressed with ~500 lb-f and placed on top of the discs before running the furnace. The product before and after the furnace treatment can be seen in Figure 8.2 for the 1000°C treatment temperature.

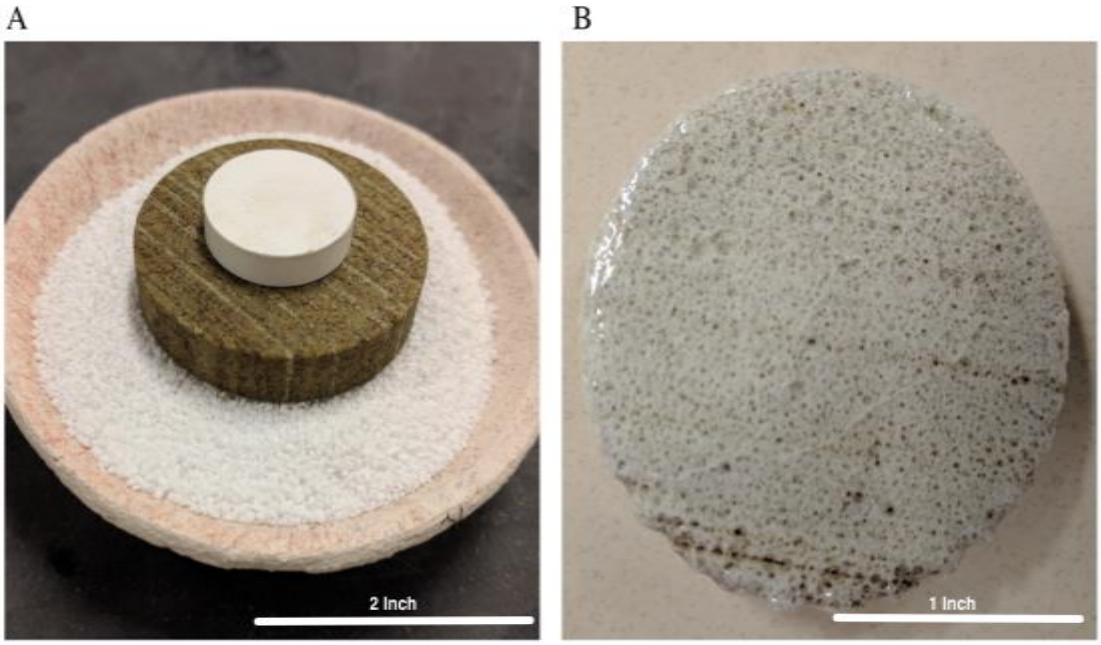

Figure 8.2 1000°C Temperature Determination Experiment. A) Before placing the sample in the furnace. B) The glass formed after the furnace

The furnace was heated directly to a peak temperature at a rate of 5 °C/min. The discs were held at their respective temperatures for 5 hr and then allowed to cool naturally to room temperature within the furnace. These experiments were raised to a peak temperature of 700°C, 715°C, 725°C, 800°C, 850°C, 900°C, and 1000°C. Table 8.1 summarizes these trials.

Table 8.1 Temperature Determination Programs

Peak Temperature (°C)	Ramp Rate (°C/min)	Hold Time (hours)
700	5	5
715	5	5
725	5	5
800	5	5
850	5	5
900	5	5
1000	5	5

After cooling, the discs were cut to analyze the depth of the borax penetration and the stability of the glass. The samples were soaked in deionized water at room temperature (~25ºC) for 12 hr and studied under the microscope to for empirical evaluation of the solubility in water. In addition, the 1000°C sample was studied using scanning electron microscopy (SEM) with energy dispersive microcopy (EDS). The 1000°C peak temperature formed the most stable glass and the temperature program was used to react the borate with the full Berea sandstone core to form a glass seal.

8.4. GLASS CORE REACTION

To prepare the core sample for the glass reaction, the unreacted core was first saturated using the boiling method described in Section 7.2.3. The core was boiled in a 27 wt. % solution of borax for approximately 5 hours. After the saturation, the sample was weighed and placed into a 110°C oven. The sample was weighed periodically until no change in weight was found to ensure dryness. The sample spent a total of 5 days in the oven. The value was taken to be the dry post-saturated weight.

Then, a borax pellet of about 5 g was pressed and placed on the sand face of the upright core in the furnace. The furnace ramped to 725°C at a rate of 3°C/min where it was held for 1 hr. It was then ramped to 1000°C at a rate of 3°C/min where it was held for 5 hr and allowed to cool naturally within the furnace to room temperature. Unlike the sandstone disc, the core was ramped at 3°C/min instead of 5°C/min. Since the core was larger, ramping it slower could mitigate cracks from thermal stresses. The sample was held at 725°C before it was brought to 1000°C to ensure that the system was in thermal equilibrium. There was also potential for more water to be trapped in the core than in the disc. Upon vaporization, gas expansion would induce greater stresses in the sample. A slower ramp rate helped alleviate potential mechanisms for cracks and fractures.

8.5. REACTED CORE PERMEABILITY MEASUREMENT

After the reacted core was removed from the furnace, it was placed into the core holder with a confining pressure of 500 psi. Unlike the original permeability procedure, this core sample was dry and did not undergo the brine saturation step. A 1% brine solution was pumped through the sample. The flow rate was set to 6 ml/min and the

pressure was monitored until flow could be noted at the fluid outlet. After, the core was placed in a dryer at 110°C for 24 hr and then saturated using the vacuum method with a 1% solution of brine. Core permeability was then measured with a wet, brine-saturated core with flow rates from 6 ml/min to 2 ml/min.

9. RESULTS

The following section reviews the findings from the experimental work.

9.1. MINERALOGY

The XRD results can be seen in Figure 9.1. The XRD yielded 96 wt. % of quartz and 4 wt. % of kaolinite.

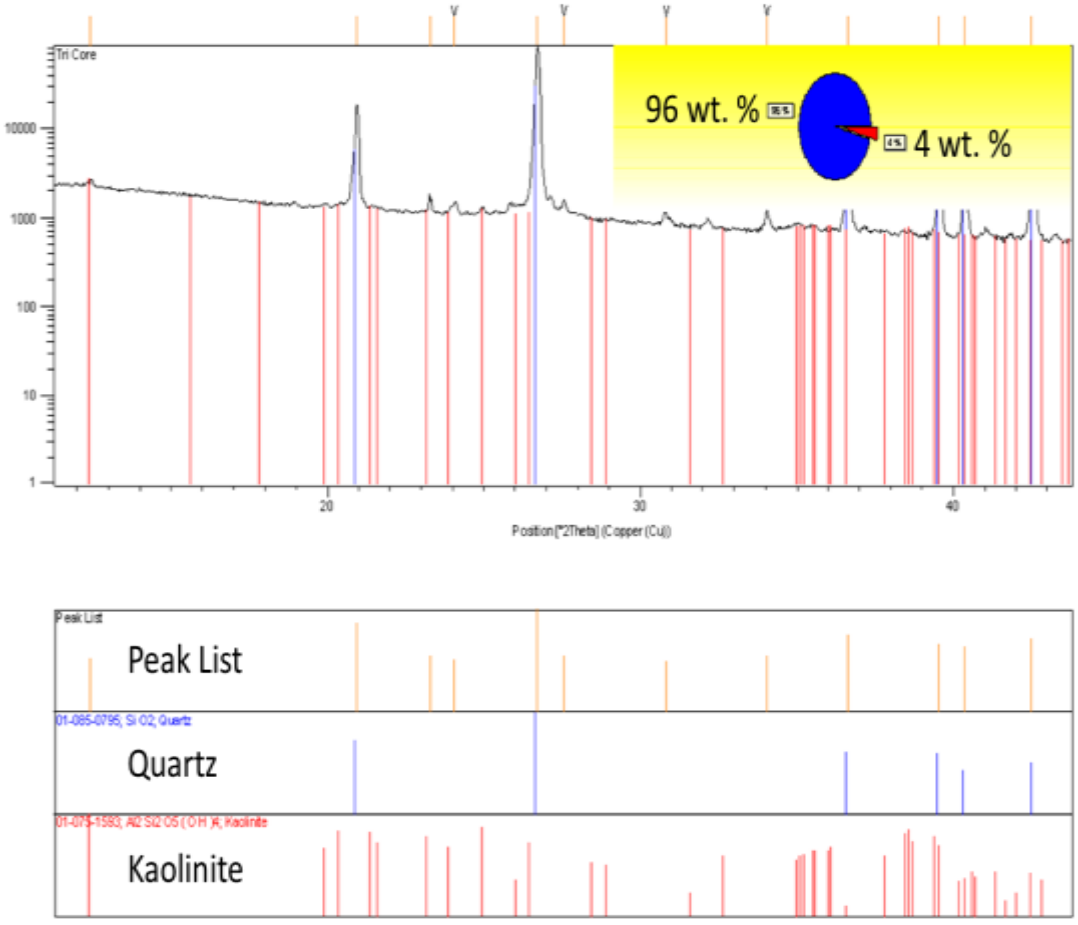

Figure 9.1 Berea Sandstone XRD

9.2. TREATMENT DETERMINATION BY DISSOLUTION

At the temperatures tested in Table 8.1, the borax was not able to melt completely until 725°C. Between 800°C, 850°C, and 900°C, there was visually observed difference noted among the quality of the glass formed on the end of the disc. To help draw a clear comparison by qualitative analysis, only the 725°C, 850°C, and 1000°C samples will be analyzed and compared. In this section, the samples of different peak temperatures were analyzed with a Leica S8 APO microscope mounted with a Leica EC3 camera after soaking the sample in distilled water at 25°C in 4 hr intervals.

Figure 9.2 is a representation of the sandstone disc after heat treatment. The disc has been cut to provide a cross-section to visualize the thickness of the glass product and the penetration depth.

Figure 9.2 Sandstone Disc Cross Section View

Figure 9.3 shows the disc top view (A through D) and corresponding cross-section views (E-H) at 0, 4, 8 and 12 hours of soak time in room temperature deionized water for samples reacted at 725°C. As shown, there was clear formation of glass on the sand face and a reaction below the sand face for the 725°C reaction. The reaction layer can be noted by the opaque layer above and the white layer below the grains. Based on

the properties of sodium borate, the less reacted and less durable glass will be more soluble in water after the thermal treatment. Borate units are susceptible to electrophilic as well as nucleophilic attack and can be hydrolyzed in both acids and bases (Bunker, 1994).

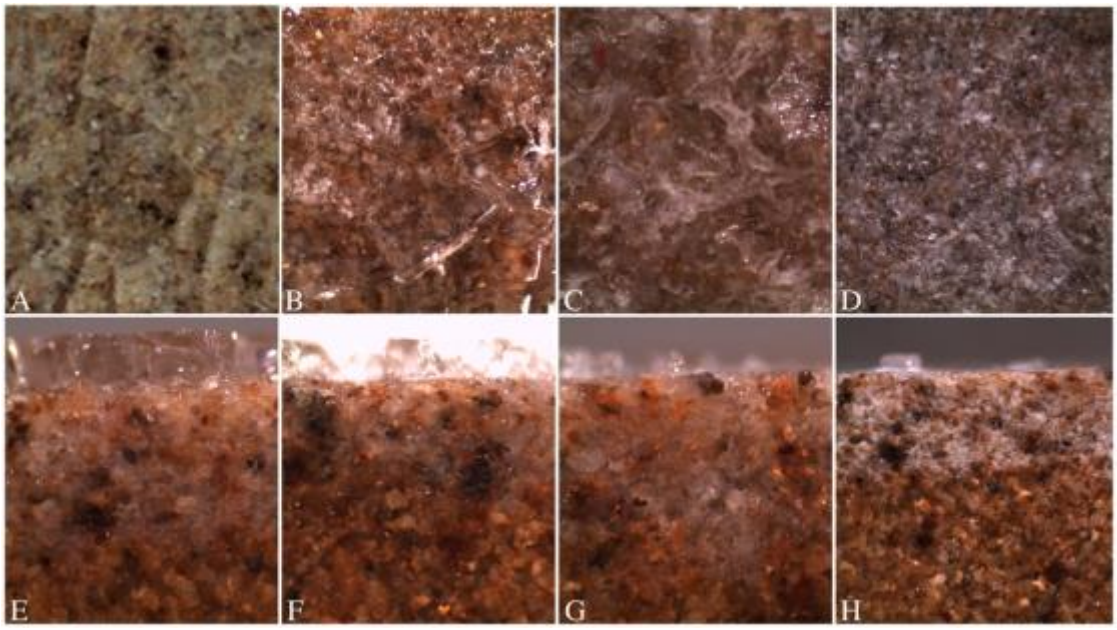

Figure 9.3 725°C Water Dissolution Test. The top row depicts a top view of the glass. A) 0 hr B) 4 hr C) 8 hr D) 12 hr. The bottom row depicts a cross section view of the glass reaction. E) 0 hr F) 4 hr G) 8 hr H) 12 hr

Comparing the 0 hr column (Figure 9.3A and 9.3E) and 4 hr columns (Figure 9.3B and 9.3F), there was a noticeable dissolution occurring at the surface. The surface of the 0 hr photo exhibits noticeable cracks due to thermal stresses from cooling. The 4 hr surface photo reveals dissolution occurring inward from these cracks as more fractures have formed and further widened. The 4 hr cross sectional image shows recession in border defining the reaction's penetration depth. The 8 hr (Figure 9.3C and 9.3G) and 12

hr of dissolution (Figure 9.3D and 9.3H) photos, the same trend was noted. The surface glass dissolved further, leaving behind small islands in the 8 hr photo, and by the 12 hr photo, the surface glass has almost completely dissolved. Looking at the cross section of the 8 hr photo (Figure 9.3G), the penetration depth was similar to that of Figure 9.3E. The photo was taken in a portion where there was greater initial penetration into the sandstone. By the 4 hr mark, the recession was less than that seen in the 0 and 2 hr due to its initial starting point. Looking at the 12 hr cross section, there was a distinct border separating the penetration of the glass reaction and the natural, unreacted sand grains. The white color of the glass was the most faded here, but the penetration border was the most distinct. Figure 9.4 gives various depths of penetration for the glass reaction and the thickness of the top layer on the sand face to compare 0 hr in deionized water to 12 hr.

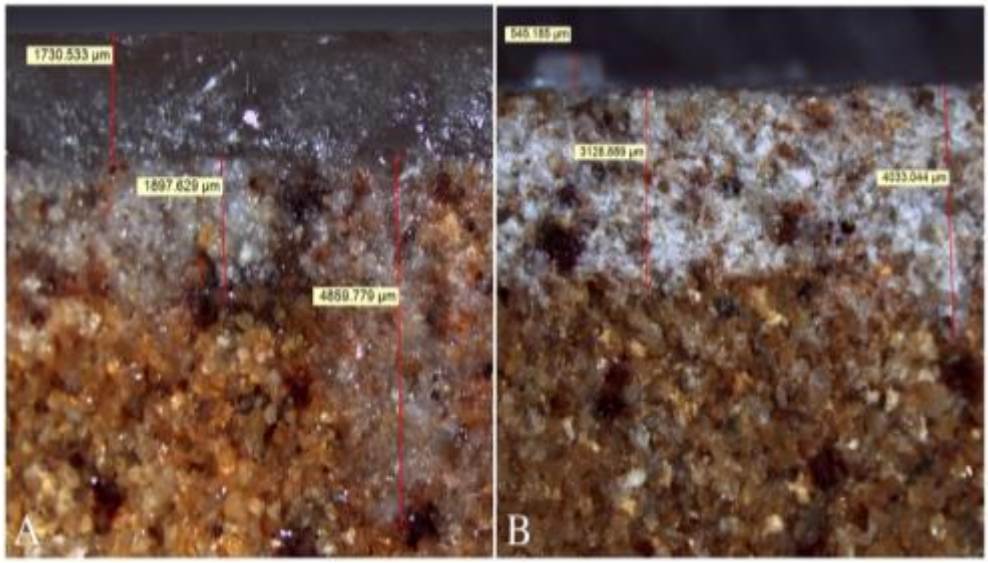

Figure 9.4 725ºC Glass Thickness. A) Cross section at 0 hr. B) Cross section at 12 hr. A and B use different scales

The surface layer dissolved from an approximate thickness of about 1.7 mm to about 0.5 mm. While the penetration depth was uneven, the maximum degree of penetration receded from about 4.8 mm to 4 mm. Considering the maximum depth of penetration, the recession trend was further supported by measurement and color density.

Figure 9.5 shows the disc top view (A-D) and corresponding cross-section views (E-H) at 0, 4, 8 and 12 hours of soak time for samples reacted at 850°C. Comparing Figure 9.5's top views (A-D) with the respective top view of Figure 9.3A-D, the surface glass quality of the 850°C samples was greater than that of the 725°C. The layer was clearer with fewer fractures. Going from 0 to 12 hr in Figure 9.5, the surface fractures widen, but the surface layer remains after the 12 hours of dissolution (unlike the 725°C where it disappears completely). Looking specifically at the 12 hr surface in Figure 9.5D, a degree of opaqueness develops as the surface begins to dissolve.

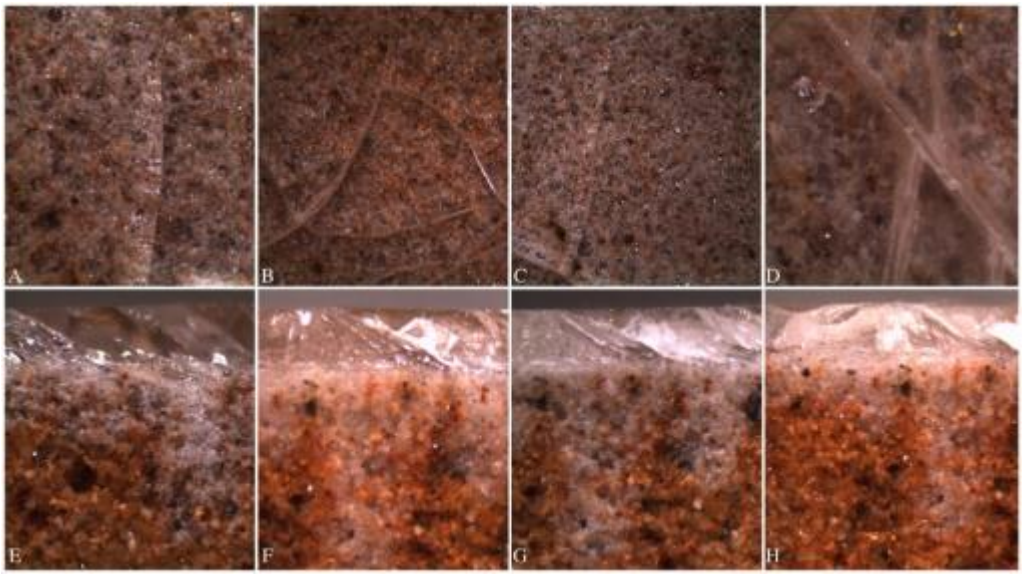

Figure 9.5 850ºC Water Dissolution Test. The top row depicts a top view of the glass. A) 0 hr B) 4 hr C) 8 hr D) 12 hr. The bottom row depicts a side view of the glass reaction. E) 0 hr F) 4 hr G) 8 hr H) 12 hr

For Figure 9.5's bottom row depicting the penetration, the glass was of higher durability also. There was no noticeable fading or receding as seen in the 725°C reaction. Yet, one should note the penetration was quite uneven and shallower than that seen on the 725°C reaction for some parts. The penetration for the 850°C reaction was quite uneven. Figure 9.6 has a surface thickness of about 1.4 mm at 0 hr and 1.2 mm at 12 hr. In Figure 9.6A, the maximum depth of penetration was 6.8 mm and the minimum depth was 2.0 mm at 0 hr. Looking at Figure 9.6B, the maximum depth was about 5.9 mm and minimum was about 1.8 mm. The recession trend was also noted here but to a lesser degree as there was less of a difference between the maximum and minimum depth after 12 hr in water.

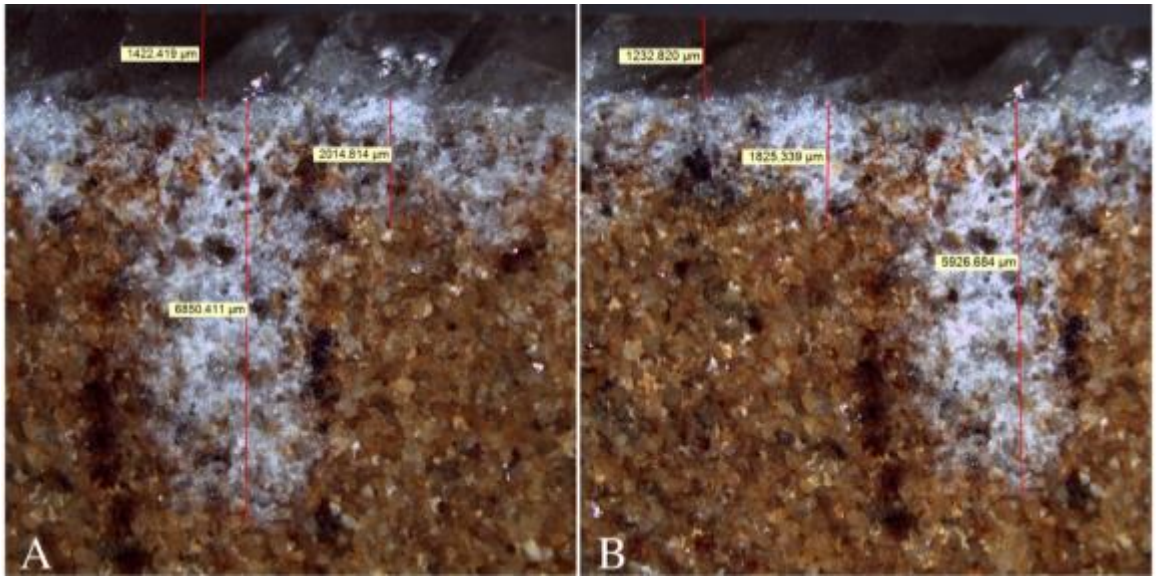

Figure 9.6 850ºC Glass Thickness. A) Cross section at 0 hr. B) Cross section at 12 hr

Figure 9.7 shows the core end view (A-D) and corresponding cross-section views (E-H) at 0, 4, 8 and 12 hours of soak time in distilled water for samples reacted at

1000°C. Comparing the glass in Figure 9.7 for the 1000°C reaction to results shown in Figures 9.3 and 9.5, the 1000°C was the most stable. Stress fractures incurred during the cooling process can be on the surface of each sample shown in Figure 9.7A-D. Yet after even 12 hours in water, the glass showed no sign of further dissolution or development of new cracks. An interesting note was the formation of relatively large (1 mm) bubbles in this reaction that were not present in either of the other two sets of samples prepared at 725°C and 850°C.

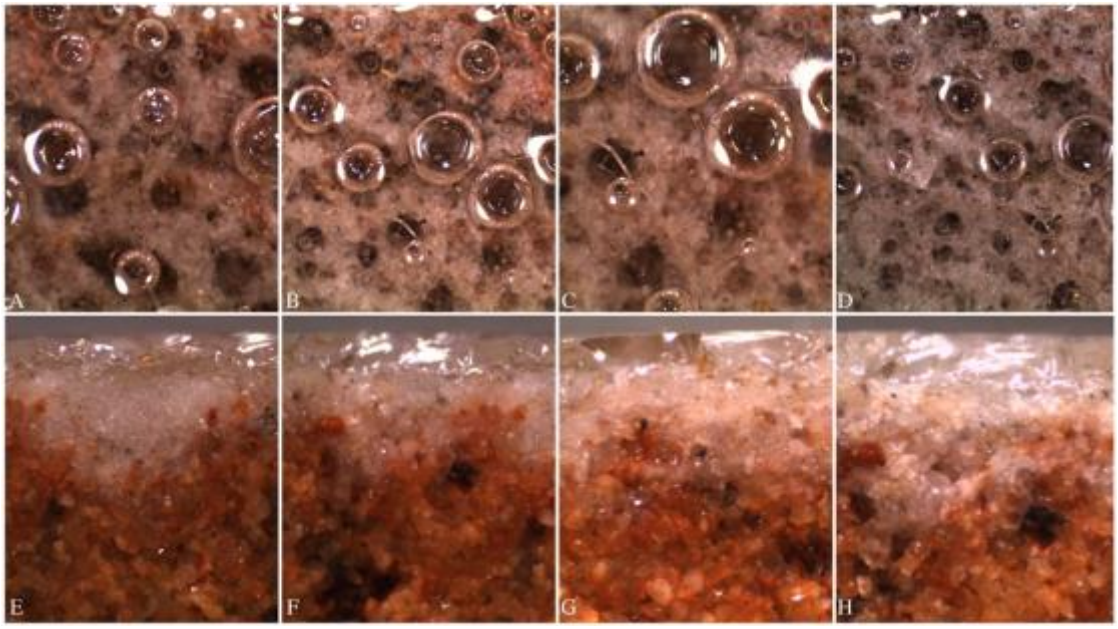

Figure 9.7 1000ºC Water Dissolution Test. The top row depicts a top view of the glass. A) 0 hr B) 4 hr C) 8 hr D) 12 hr. The bottom row depicts a side view of the glass reaction. E) 0 hr F) 4 hr G) 8 hr H) 12 hr

There was some type of gas escaping the pores at this temperature coupled with a lowered glass viscosity that allows for the large bubble formation. At the peak temperature, all the water should have already been vaporized. Looking at the glass layer

below the sand face in Figure 9.7E-H, the penetration was quite even throughout. Also, the glass shows no sign of color fading or penetration recession. The penetration was not as deep as that seen in the 850°C reaction, but it was distributed more evenly. The color density of the glass formed for the 1000°C reaction was higher than that of the 725°C and 850°C from the white color.

Figure 9.8 depicts the glass thickness for the 1000ºC reaction. The surface thickness was about 0.4mm at 0 hr and 0.5 mm at 12 hr. Since the starting and end points for the measurement were marked by eye, there was a potential source for human error in these measurements.

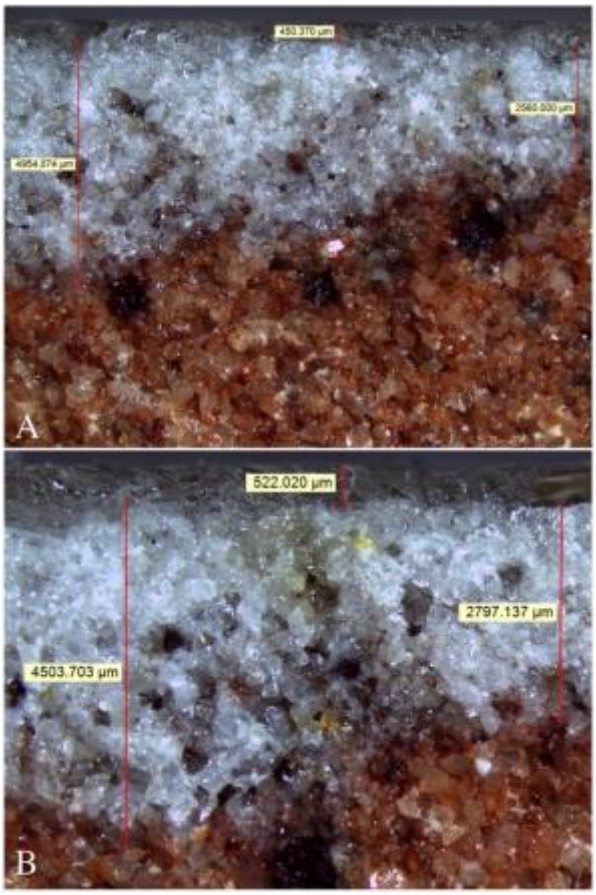

Figure 9.8 1000ºC Glass Thickness. A) Cross section at 0 hr. B) Cross section at 12 hr

The increased thickness may be due to a thicker portion at that section of the specimen or an error with the starting and end points for the marks. The maximum penetration depth at 0 hr was about 4.9 mm and the minimum was about 2.5 mm. After 12 hr, the maximum was about 4.5 mm and the minimum was about 2.7 mm. Although the section spent time in water and the maximum depth marks follow the recession trend noted in other samples, the sign of elongation due to errors can be seen as promising. At best, these values can represent minimal or almost no recession. Based on the durability and penetration depth distribution, the selected reaction peak temperature was 1000°C for the full core reaction of the study.

9.3. SEM-EDS RESULTS

This section analyzes the glass reaction in a semi-quantitative manner using energy dispersive spectroscopy (EDS) from the sodium content in the reacted sample. Only the EDS for the 1000°C sample will be reported since it was determined to be the preferred reaction temperature. The EDS measurement for the 725°C and 850°C reaction yielded similar results and denoted the same trend as seen by the 1000°C sample. The EDS was studied qualitatively to detect a trend in the oxygen, sodium and silicon content. Sodium was not present in the Berea sandstone. The sodium was introduced by the borax. The silicon came from the SiO_2 from quartz in the Berea sandstone sample. Figure 9.9 from left to right depicts the EDS for the sandstone, sandstone-glass interface, and glassy product from the reacted borax. Examining three elements oxygen (O), sodium (Na), and silicon (Si), a simple trend can be noted. The oxygen was abundant in all three frames. Moving from the grains, to the interface, and then to the glass, the

sodium content increases. Conversely, the silicon content decreases moving from the sandstone, to the interface, and then to the glass.

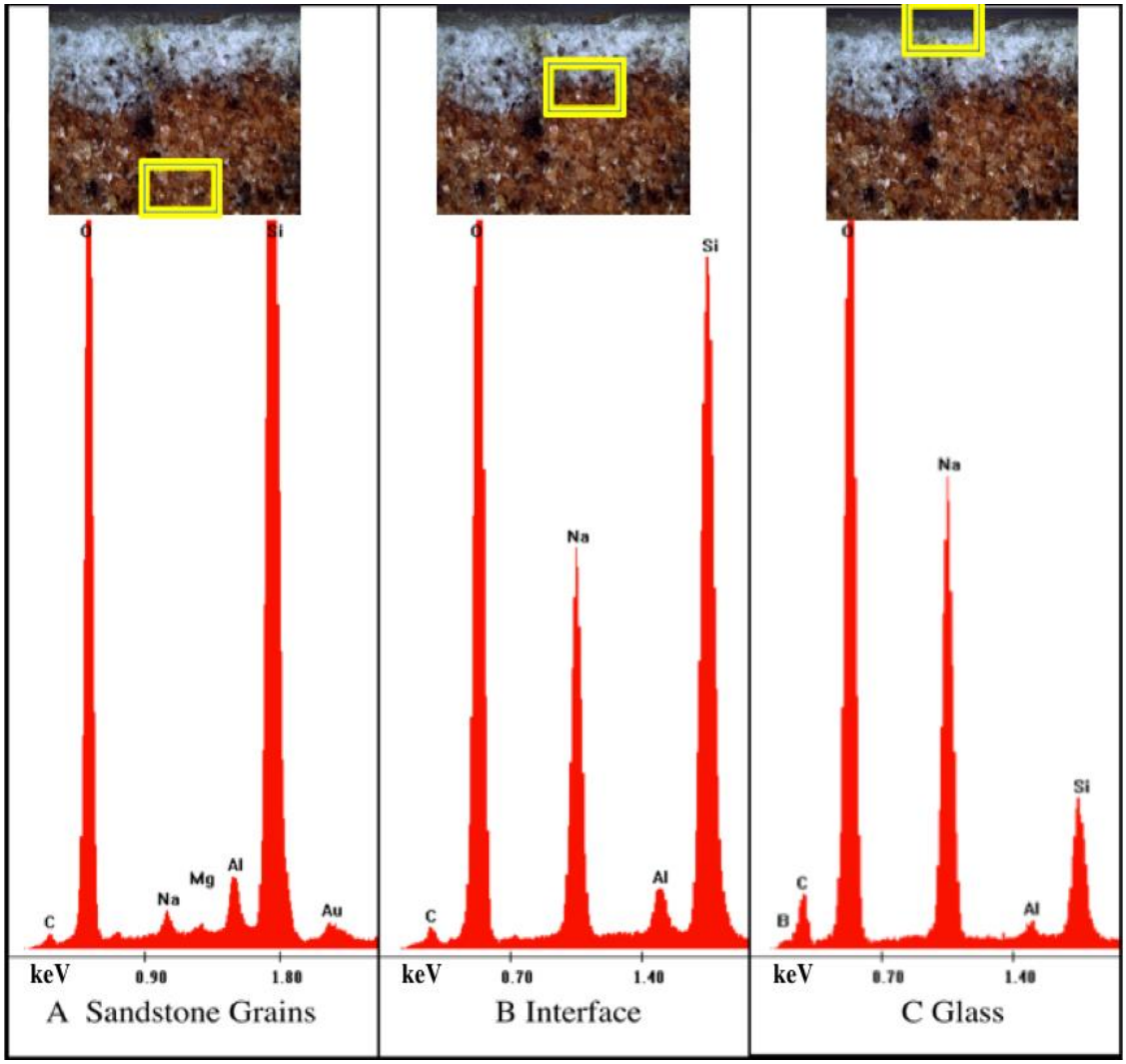

Figure 9.9 1000ºC EDS Spectra Readings

The SEM photo from Figure 9.10A reveals a cross sectional image of the glass that formed on the sand face. Figure 9.10B reveals a cross sectional image that includes the glass-sandstone interface and sandstone grains. Figure 9.10B was positioned such

that the surface glass was not shown. The very top of Figure 9.10B captures the where the sand face begins where the Na_2O-$2B_2O_3$ melt enters the formation. Moving downward from the top of Figure 9.10B, there should be the glass reaction product, glass interface, and then sand grains layer.

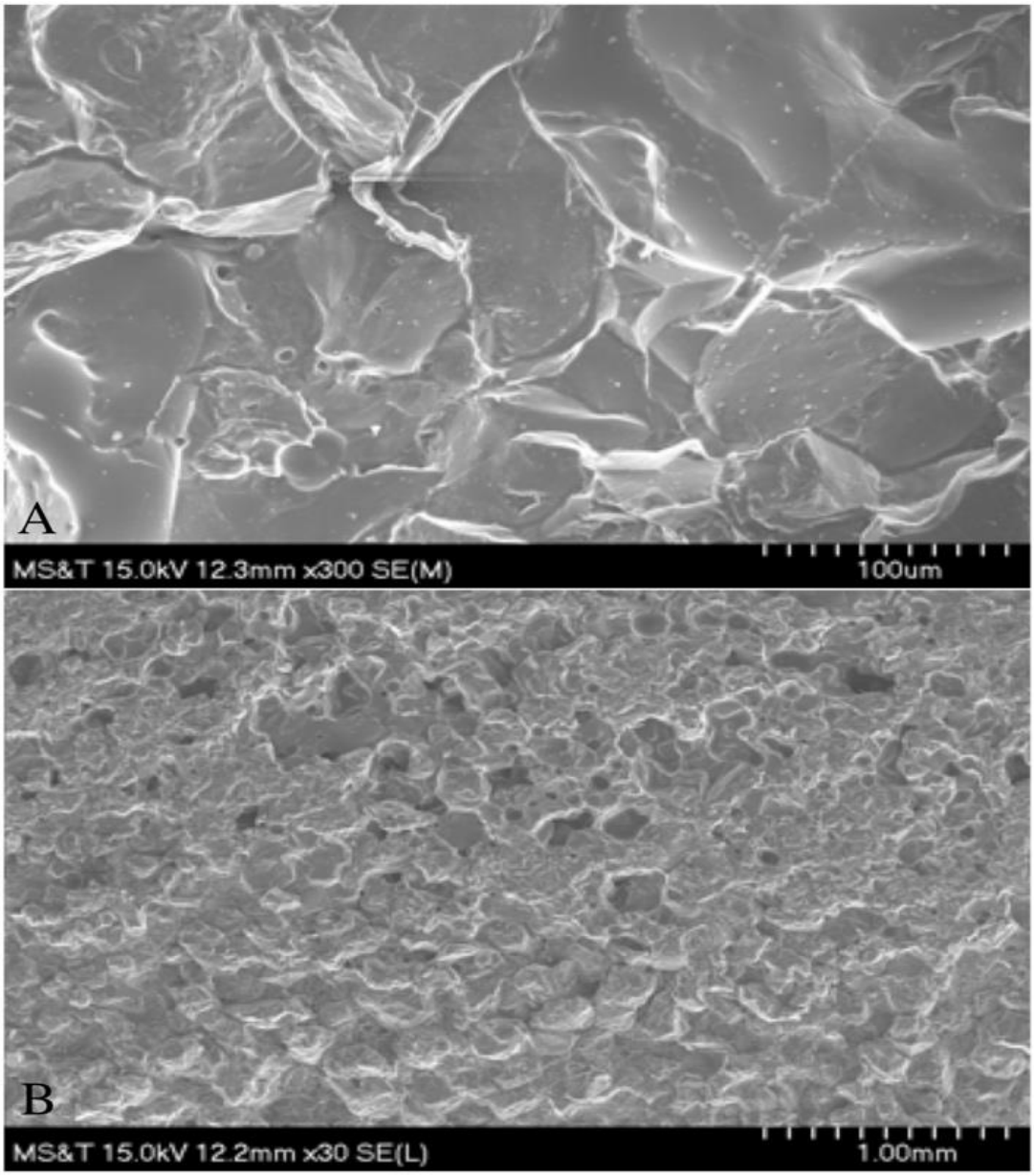

Figure 9.10 1000ºC SEM Cross Section Image. A) Upper Glass Layer. B) Reacted Glass-Grain Interface

9.4. UNREACTED CORE MEASUREMENTS

Data gathered for the unreacted core is summarized in Table 9.1.

Table 9.1 Unreacted Core Measurements

Dry Weight (g)	539.73
Brine Saturated Weight (g)	587.00
Length (cm)	12.00
Diameter (cm)	5.01
Cross-sectional Area (cm^2)	19.71
Bulk Volume (cm^3)	236.56
Pore Volume (cm^3)	47.27
Porosity (%)	0.20

The difference in the dry versus brine saturated core weight gave a pore volume, 47.27 cm^3. Given the bulk volume derived from the volume measurement of the core, the fraction between the pore volume and bulk volume, 236.56 cm^3, equals a porosity of about 20%. Using the viscosity, area, and length data for a given flow rate, Table 9.2 was created to determine the permeability of the core sample with Darcy Law (Equation 2). The variance among each permeability measurement was quite small with a 2.46 standard deviation. The average permeability measurement was 95.01 mD for the core sample.

Table 9.2 Unreacted Permeability Determination

Brine Injection		
q (ml/min)	**ΔP (psi)**	**K (mD)**
2	3	99.42
3	4.7	95.19
4	6.4	93.21
5	7.9	94.39
6	9.2	97.26
Permeability Average	**95.01 mD**	
STD	**2.46**	

9.5. REACTED CORE MEASUREMENTS

A core weighing 539.73 g was saturated in a 27 wt. % solution of borax. The difference between the dry weight and the borax saturated weight was 51.37 g—the weight of the borax solution occupying the pore space. An estimate yields that approximately 13.87 g of borax was deposited into the pore space since 27% of the solution comprised of borax. After 5 days in a 110ºC oven, the core weighed 550.50 g, and it was assumed to be dry. The weight increased by 10.77 g. A borax pellet was placed on this sample and run with the 1000ºC program determined from Section 9.2. After the glass formation reaction, the reacted core was flooded with a solution of 1% brine to determine a pressure value where flow can be noted. The reacted core was not saturated and was placed into the core sleeve dry. Flow was noted at 24 psi. Looking at

Table 9.3, the brine saturated glass core had its permeability measured. The standard deviation between the permeability measurement was miniscule at 0.07. The measured permeability was 5.16 mD. Comparing it to the original, the average permeability, 5.16 md, yielded a 94.57% reduction from the unreacted sandstone permeability, 95.01mD.

Table 9.3 Reacted Permeability Determination

Brine Injection		
q (ml/min)	**ΔP (psi)**	**K (mD)**
2	56.5	5.28
3	85.5	5.23
4	115.4	5.17
5	144.6	5.16
6	175.5	5.10
Permeability Average	**5.16 mD**	
STD	**0.07**	

Table 9.4 summarizes the pressure differentials of both the unreacted and reacted core flooding experiments, along with a computed plugging factor. The plugging factor represents the ratio of the new pressure differential to the old pressure differential as seen in Equation 3.

Table 9.4 Plugging Factor Determination

q (ml/min)	ΔP (psi) Reacted	ΔP (psi) Unreacted	Plugging Factor
2	56.5	3.0	18.83
3	85.5	4.7	18.19
4	115.4	6.4	18.03
5	144.6	7.9	18.30
6	175.5	9.2	19.08
Average Plugging Factor	**18.49**		
STD	**0.45**		

The plugging factor is defined as the post reaction pressure divided by the pre-reaction pressure. The plugging factor of 18.49 means that the system requires 18.49 times the old pressure to exhibit the same flow rate. The experiment yielded average value of 18.49 for the plugging factor and 0.45 as the standard deviation.

$$Plugging\ Factor = \frac{\Delta P_{Final}}{\Delta P_{Initial}} \qquad (3)$$

After the permeability experiment, the reacted core was cut to examine the depth of penetration for the glass reaction as seen in Figure 9.11. Figure 9.11A is a picture of the unreacted core, and Figure 9.11B is an end view of the core sand face. Figure 9.11C depicts the penetration depth of the borax pellet ranging from about 1.4 mm to 2.5 mm.

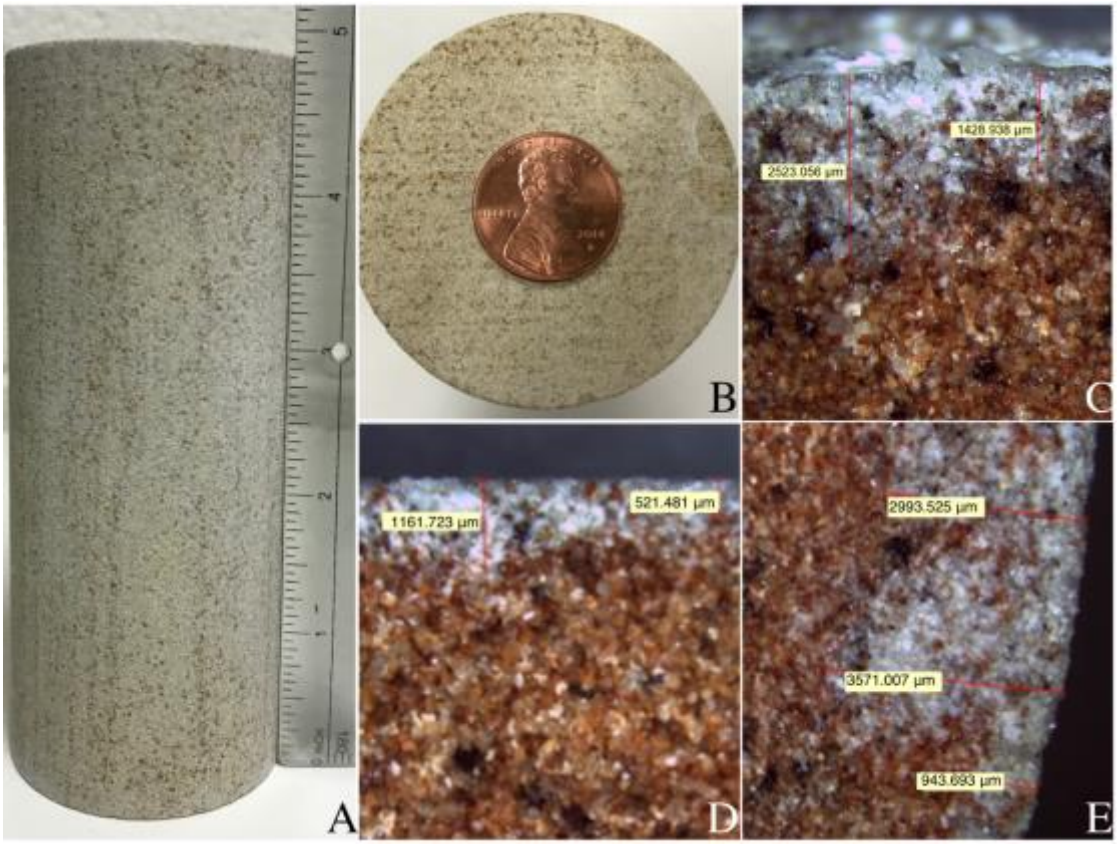

Figure 9.11 1000ºC Reacted Core Sections. A) Side of the unreacted Berea sandstone core B) Top view of the unreacted sandstone. C) Transverse cross section of the borax pellet reacted core end. D) Medial cross section flow experiment. E) Transverse cross section opposite the pellet reacted end

Since the permeability of the reacted core was tested, the glass cap dissolved from exposure to the brine solution. No measurement for the thickness was determined for the upper glass layer covering the sand face in 9.11C. Figure 9.11D is a cross sectional image of the core end opposite to the borax pellet reaction end. A glass reaction occurred here due to the saturation in a borax solution. The depth of penetration varies from about 0.5 mm to 1.1 mm. Figure 9.11E is a medial cross section to examine the lateral penetration depth. The penetration depth varies from about 0.9 mm to 3.5 mm. The borax was deposited laterally into the core saturating the sample by boiling in borax.

As shown in Figure 9.12, the reacted core formed a solid seal on the sand face.

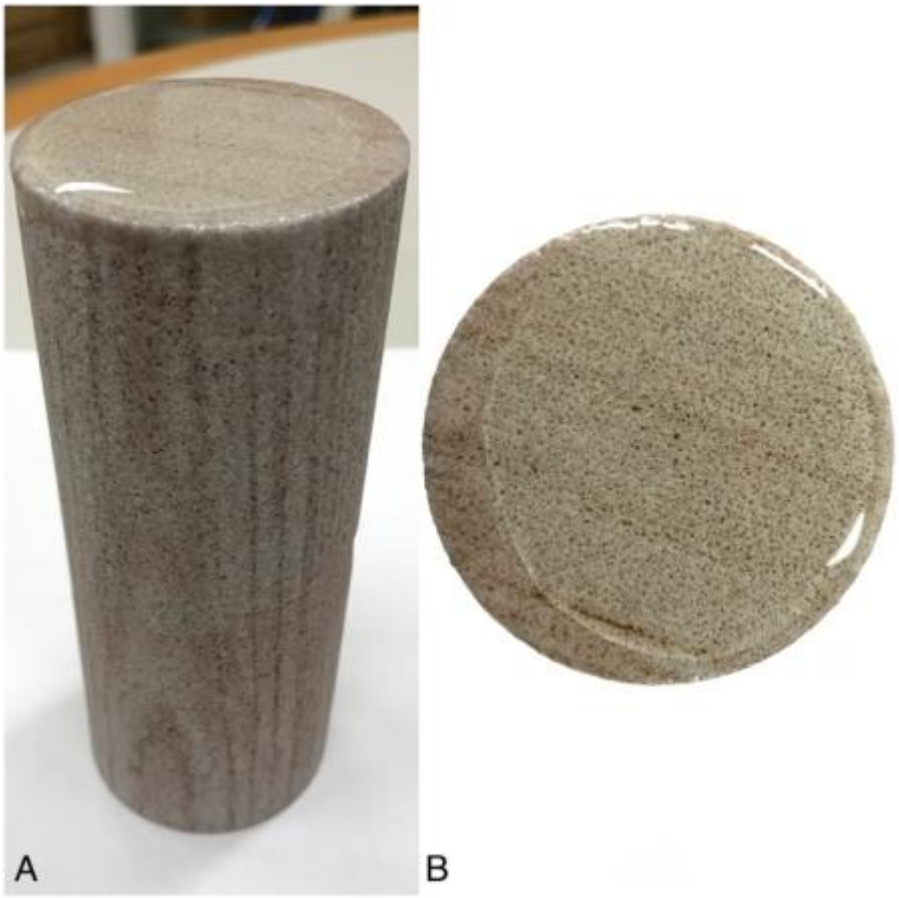

Figure 9.12 1000ºC Reacted Core. A) Angled View. B) Top View

Figure 9.12B shows very few cracks aside from a curve fracture in the shape of a half circle around part of the glass face. Unlike the disc from Figure 9.7, no large bubbles formed. Since the core was ramped at a slower rate and held at 725°C before reaching the peak temperature of 1000°C, the product may not resemble that of the sample from Figure 9.7. The change in program may have caused the viscosity of the melt form Figure 9.12 to be lower, allowing gas to escape from solution. Also unlike the surface

glass layer seen in Figure 9.7B, the glass layer in Figure 9.12B was soft to feel. The top most glass layer was most likely Na2O-2B2O3 glass containing no or very little SiO_2. The highly soluble glass was removed by water dissolution. Unlike the 725°C disc in water, a hard solid layer of glass remained. The glass in Figure 9.11C dissolved glass layer on the sand face no longer had a soft feel.

10. DISCUSSION

Amongst the three studied temperatures (725°C, 850°C, 1000°C), a glass coating that penetrated into the sandstone core, with variable composition was formed. The product had a gradient with increasing SiO_2 content closer to the formation. Figure 10.1 provides an alternative view of the reaction.

Figure 10.1 1000ºC Reaction Profile

From dissolutions over a given time period, the glass thickness on the surface and the penetration depths were studied. There was evidence that the top layer was simple a sodium borate glass (without silica) while the penetrated Na_2O-$2B_2O_3$ melt reacted to form a borosilicate glass. This theory was the most plausible in the 725°C reaction due to the complete dissolution of the top layer. Looking at the 850°C and 1000°C reaction, both top layer and penetrated layer were almost completely undissolved after 12 hr in deionized water. This suggest a more durable glass formed. Looking at the EDS for the 1000ºC specimen, some quality of silicon was detected in each of the three layers. This was notable particularly in the glass layer at the surface. The pellet placed on top was

borax, that contains no silicon. The silicon EDS reading suggest that even the top layer reacted with silica from the sandstone. Moving into the interface and sandstone grains, one can note the decreasing sodium content. Since the source of sodium originated from the borax pellet, it was expected to see this decrease, as one moves from the top glass layer, through the interface, into the natural sandstone sample. Since the silicon originates from the sandstone grains, it was more surprising to see it in present in the top glass layer suggesting a reaction between the two (even away from the source of silicon). Comparing the 12 hr surface of the 850°C and 1000°C, the 850°C developed an opaque sheen as the surface began to dissolve away. Such a phenomenon was not witnessed in the 1000°C, further supporting the strong durability of the formed glass in both the upper and lower layer. Thus, 1000°C was the choice for the experiment's peak hold temperature.

The SEM image from Figure 9.10 proved to be somewhat difficult to analyze. Since the pieces were not polished, it was challenging to differentiate the glass layer from the sandstone grains. The Figure 9.10A was taken quite close to the surface of the profile to ensure that it was centered on the glass. Note the conchoidal fractures from cutting the piece that were characteristic of glass fracturing. Looking at Figure 9.10B provides a challenge. The spherical grains and filamentous connections make it challenging to denote the exact area of the glass to sand grain interface. Polishing the samples would help visualize these areas better for future reference.

The reacted core underwent a 94.57% permeability reduction from the original sandstone sample measurement. Although the formed glass did not prevent flow completely, the large reduction in permeability was promising and yields potential for

future study. The glass seal that formed on the pellet side of the core created a semi-permeable medium. Due to the cracking from thermal expansion shrinkage, the glass seal may lose some integrity during its initial formation process. Images from Figure 9.12 depict a soft finish to the glass face unlike that seen in the glass disc reactions for temperature determination. The reaction for the core was run at a slower ramp rate with a hold time at 725°C and 1000°C to increase the reaction time. This helped ensure that the core larger system heat thoroughly. This change in the program may attribute to the difference in glass quality, as the glass layer saw dissolution for the core top surface but not the disc. One can note the formation of a borosilicate glass within the formation itself below the sand face. It was difficult to quantify the respective seal contributions from the surface glass to the penetrated glass. Yet, the results provide evidence that glass can be formed with the sandstone grains and form a durable bond and material.

Looking at the samples in Figure 9.11C, the penetration of the Na_2O-$2B_2O_3$ melt into the sample was quite shallow as it varied from 1.4 mm to 2.5 mm. Although 2.5 mm was not deep, the glass formation contributed to almost a 95% reduction in the permeability. The top glass layer on the core could not be measured. The sample was exposed to water and the soft glass dissolved leaving behind a thin layer that could not be measured like the disc samples. Looking at Figure 9.4A, 9.6A, and 9.8A, the top glass layer's thickness decreased as the maximum hold temperature increased. Respectively, the thicknesses were 1.7 mm, 1.4mm, and 0.4mm before soaking in water. If the glass top was thicker on the core, the glass on top would likely contain less silica and be more soluble. This trend held true with the dissolution studies. Given the dissolution results of the core, it was more likely that the glass thickness was closer to 1.7 mm rather than 0.4

mm. Figure 9.11D and 9.11E show the depth of penetration of the Na_2O-$2B_2O_3$ laterally into the core and into the bottom end (opposite to the pellet reacting face). This borax was introduced from boiling in a 27 wt. % solution. The greatest penetration varied from 0.5 mm to 3.5 mm. Although it was estimated that a sample of about 10.77 g of borax was deposited into the sample, this lack of penetration deeper into the sample suggests that the borax solution did not saturate the sample completely.

The plugging factor averaged 18.49 for the reacted core. This plugging factor is a useful quantification outside of permeability to determine the folds of increase in the pressure required to see flow through the core. This measurement provides a means to compare the effectiveness of other plugs and other glass reactions in the future.

11. CONCLUSION

This work explored the possibility of glass as a plugging material in sandstones, with a view toward applying the method as an abandonment material for wells in the oil and gas industry. Utilizing a simple approach of placing borax on a sandstone core, the project forms a layer of borosilicate glass with a gradient composition on both the surface of the core and in its near surface pore space. Conclusions of this study:

I. The experiment successfully formed a glass that was both fused to and part of the sandstone formation sample.

II. The glass formed on both the sand face and sides of the core with relatively shallow penetration of 1.4 mm to 2.5 mm into the sand face.

III. The experiment was successful in reducing the permeability of the sandstone by about 95% for an average permeability of 5.16 md.

IV. Although a fully impermeable seal was not created, the large reduction in permeability is encouraging and suggests additional work.

12. FUTURE WORK

The foremost area to move forward in lies with the permeability alteration of the glass. To create a plug that reduces the permeability by virtually 100%, the project must explore manners to form a more solid seal that penetrated further and more uniformly into the formation sample. One can investigate saturating the core using a vacuum method. Other possibilities may include boiling for longer periods of time to better achieve 100% borax solution saturation. Yet, the porosity structure of the sample may be a limiting factor instead of time spent boiling. Keeping in mind the literature review and similar projects already conducted, utilizing a heating element with raw glass materials has potential to form a thicker layer with deeper penetration due to creation of molten material.

Looking at the glass properties itself, the glass composition was not explored in detail for this project. By altering the composition of the raw material to balance the reaction, one can achieve more desirable coefficients of expansion that better transition into the formation's coefficient and reduce the likelihood of fractures or debonding. Looking at the phase diagram, borax in contact with the sandstone allows a glass to be formed at a lower temperature than the melting point of Na_2O-B_2O_3. Soda ash alone would lower the melting temperature, but the glass product has with poor durability. Exploring a range of compositions (families) of borosilicate glasses could yield desirable properties for a plug. Other silicate based glass compositions may melt at a reasonable temperature and produce durable glasses. This project studies glass formation in a sandstone formation. There is opportunity to explore other formation types which would create different types of glasses depending on the minerology. The mechanisms and rate

of glass degradation under wellbore conditions opens the door to a world of possibilities. Varying the heat, pH, presence of various ions, gases, and chemicals, in addition to thermal and pressure cycles, are all directions to take this project.

A more thorough experiment can be conducted to study the mechanical and chemical properties of the formed glass. The projected explored permeability and water solubility. Further studies can be conducted to explore the glass properties and its behavior in the pore space, bound to the formation, and how outside forces can impact the material.

REFERENCES

Arnold, K., Clegg, J. D., Fanchi, J. R., Holstein, E. D., Lake, L. W., F., M. R., & Warner, H. R. (2006). *Petroleum Engineering Handbook*. Richardson, TX: Society Of Petroleum/Engineers.

Bazargan, M., Soliman, M., Habibpour, M., & Rezaei, A. (2014). Plasma Torch Perforation to Route Hydraulic Fracturing Operation in Unconventional Reservoirs (Vol. 3, pp. 2083–2091). American Rock Mechanics Association.

Bellarby, Jonathan. *Well Completion Design*. Amsterdam: Elsevier Science, 2009. Print.

Bois, A., Garnier, A., Galdiolo, G., & Laudet, J. (2010). Use of a mechanistic model to forecast cement-sheath integrity for CO2 storage. *SPE International Conference on CO2 Capture, Storage, and Utilization*. doi:10.2118/139668-ms.

Brufatto, C., Cochran, J., Power, L. C. D., El-Zeghaty, S. Z. A. A., Fraboulet, B., Griffin, T., et al. (2003). From Mud to Cement - Building Gas Wells. *Oilfield Review*, *15*(3).

Bunker, B. C. (1994). Molecular mechanisms for corrosion of silica and silicate glasses. *Journal of Non-Crystalline Solids*, *179*, 300–308.

De Andrade, J., Sangesland, S., Todorovic, J., & Vrålstad, T. (2015). Cement Sheath Integrity During Thermal Cycling: A Novel Approach for Experimental Tests of Cement Systems. *SPE Bergen One Day Seminar*. Society of Petroleum Engineers. http://doi.org/10.2118/173871-MS

Dowdle, W., & Cobb, W. (1975). Static Formation Temperature From Well Logs - An Empirical Method. *Journal of Petroleum Technology,27*(11), 1326-1330. doi:10.2118/5036-pa.

Dump Bailer. (2017). *Schlumberger Oilfield Glossary*.

Eagan, R. J., & Swearengen, J. C. (1978). Effect of Composition on the Mechanical Properties of Aluminosilicate and Borosilicate Glasses. *Journal of the American Ceramic ...*, *61*(1-2), 27–30.

Economides, M. J., Watters, L. T., & Dunn-Norman, S. (1998). *Petroleum Well Construction*. Chichester: John Wiley & sons.

Fields, S.A., Martin M.M., 1997. The Plugging Process: Securing Old Gas & Oil Wells for the protection of the Environment. Proceedings: Decommissioning Workshop, September 1997, California, USA.

Fraser, H. (2005). *Ceramic Faults and their Remedies*. London: A. & C. Black.

Goff, S. J., Bussod, G. Y., Wohletz, K., Dick, A., & Rowley, J. C. (1994). Rock Melting: A Specialty Drilling System for Improved Hole Stability in Geothermal Wells. *World Geothermal Congress: Worldwide Utilization of Geothermal Energy*.

Goodwin, K. J., & Crook, R. J. (1992). Cement Sheath Stress Failure. *SPE Drilling Engineering*, *7*(04), 291–296. http://doi.org/10.2118/20453-PA

Gowthaman, S., Krishnya, S., & Nasvi, M. C. (2016). Effect of Salinity on Mechanical Behaviour of Well Cement: Application to Carbon Capture and Storage Wells. *Engineer: Journal of the Institution of Engineers, Sri Lanka,49*(1), 21. doi:10.4038/engineer.v49i1.6915.

Graves, R., Samih, B., Parker, R., & Gahan, B. (2002). Temperatures Induced by High Power Lasers: Effects on Reservoir Rock Strength and Mechanical Properties. Presented at the Proceedings of SPE/ISRM Rock Mechanics Conference, Society of Petroleum Engineers.

Griffith, J., Sabins, F., & Harness, P. (1992). Investigation of Ultrasonic and Sonic Bond Tools for Detection of Gas Channels in Cements. *SPE Annual Technical Conference and Exhibition*. doi:10.2118/24573-ms.

Haliburton, Erle P. Method and means for cementing oil-wells. U.S. Patent and Trademark Office, assignee. Patent 1369891. 1 Mar. 1921. Print.

Holloway, D. G. (1973). *The Physical Properties of Glass*. London: Wykeham Publications.

Hubert, M., & Faber, A. J. (2014). On the Structural Role of Boron in Borosilicate Glasses. *European Journal of Glass Science and Technology*.

IEA Greenhouse Gas R&D Programme (IEA GHG), "Long Term Integrity of CO_2 Storage – Well Abandonment", 2009/08, July 2009.

India Cements LTD. Coromandel King Oil Well Cement. Retrieved from http://www.indiacements.co.in/coromandel-king-oil-well-cement.php

Ingraffea, A. R., Wells, M. T., Santoro, R. L., & Shonkoff, S. B. (2014). Assessment and risk analysis of casing and cement impairment in oil and gas wells in Pennsylvania, 2000 2012. *Proceedings of the National Academy of Sciences,111*(30), 10955-10960. doi:10.1073/pnas.1323422111.

Jackson, P., & Murphey, C. (1993). Effect of Casing Pressure on Gas Flow Through a Sheath of Set Cement. *Proceedings of SPE/IADC Drilling Conference*. doi:10.2523/25698-ms.

Jackson, R. B. (2014). The integrity of oil and gas wells. *Proceedings of the National Academy of Sciences,111*(30), 10902-10903. doi:10.1073/pnas.1410786111.

Jacobs, T. (2017, April 1). Oil and Gas Producers Find Frac Hits in Shale Wells a Major Challenge. *Journal of Petroleum Technology,69*(04), 29-34. doi:10.2118/0417-0029-jpt.

Kang, M., Christian, S., Celia, M. A., Mauzerall, D. L., Bill, M., Miller, A. R., . . . Jackson, R. B. (2016). Identification and characterization of high methane-emitting abandoned oil and gas wells. *Proceedings of the National Academy of Sciences,113*(48), 13636-13641. doi:10.1073/pnas.1605913113.

Kellingray, D., 2007. Cementing - Planning for success to ensure isolation for the life of the well. *SPE 112808-DL, SPE Distinguished Lecturer Series* 2007.

King, G. E., & King, D. E. (2013). Environmental Risk Arising From Well Construction Failure: Differences Between Barrier Failure and Well Failure, and Estimates of Failure Frequency Across Common Well Types, Locations and Well Age. *SPE Annual Technical Conference and Exhibition*. doi:10.2118/166142-ms.

King, G. E., & Valencia, R. L. (2014). Environmental Risk and Well Integrity of Plugged and Abandoned Wells. *SPE Annual Technical Conference and Exhibition*. doi:10.2118/170949-ms.

Kocis, I., Kristofic, T., Gajdos, M., & Horvath, G. (2015). Utilization of Electrical Plasma for Hard Rock Drilling and Casing Milling. *SPE/IADC Drilling ...*. http://doi.org/10.2118/173016-ms

Laudet, J., Garnier, A., Neuville, N., Guen, Y. L., Fourmaintraux, D., Rafai, N., . . . Shao, J. (2011). The behavior of oil well cement at downhole CO2 storage conditions: Static and dynamic laboratory experiments. *Energy Procedia,4*, 5251-5258. doi:10.1016/j.egypro.2011.02.504.

Lecolier, E., Rivereau, A., Ferrer, N., Audibert-Hayet, A., & Longaygue, X. (2006). Durability of Oilwell Cement Formulations Aged in H2S-Containing Fluids. *Proceedings of IADC/SPE Drilling Conference*. doi:10.2523/99105-ms.

Li, Z., Wang, Y., Liu, B., & Yang, C. (2015). Composition Optimization of Glass-Like Casing and Its Novel Application in Mending Instable Borehole Wall. *Advances in Materials Science and Engineering,2015*, 1-7. doi:10.1155/2015/945475.

Lowry, W., Dunn, S., Coates, K., Duguid, A., & Wohletz, K. (2015). *High Performance Ceramic Plugs for Borehole Sealing*. *American Nuclear Society*. Charleston: International High-Level Radioactive Waste Management Conference.

Manaktala, H. K. (1992). *An Assessment of Borosilicate Glass as a High-level Waste Form*. San Antonio: Nuclear Regulatory Commission.

Morey, G. W. (1951). The Ternary System Na_2O-B_2O_3-SiO_2. *Journal of the Society of Glass Technology, 35*.

Ojovan, M. I., & Batyukhnova, O. G. (2007). Glasses for nuclear waste immobilization. *Waste Management Symposium*.

Phillips, C. J. (1960). *Glass: Its Industrial Application*. New York: Reinhold.

Rogers, M. J., Dillenbeck, R. L., & Goboncan, G. (2006). OK, We Can't Get API Cement; What Now? *SPE Annual Technical Conference and Exhibition*. doi:10.2118/102184-ms.

Schlumberger, D. (1984). *Cementing Technology*. London: Nova Communications.

Standard, N. (2004). Well integrity in drilling and well operations. *D-010*.

Technologies, C., Energy, S., Group, T. M., University of Houston. (2012). *Development of Methods to Prohibit and Remediate Loss of Annular Isolation in Shale Gas Wells: Prevention and Remediation of Sustained Casing Pressure and other Isolation Breaches*. Houston, TX: Research Partnership to Secure Energy for America.

Vignes, B. and Aadnoy, B, 2008. Well Integrity Issues Offshore Norway, SPE/IADC 112435 presented at the SPE/IADC Drilling Conference and Exhibition held in Orlando, Florida, 4-6 March 2008.

Watson TL, Bachu S (2009). Evaluation of the potential for gas and CO_2 leakage along wellbores. SPE Drill & Compl 24:115–126.

Wei, S., Jiang, Z., Liu, H., Zhou, D., & Sanchez-Silva, M. (2013). Microbiologically induced deterioration of concrete: a review. *Brazilian Journal of Microbiology,44*(4), 1001-1007. doi:10.1590/s1517-83822014005000006.

Well Plug and Abandonment. (2017). *Natural Gas Investing*.

Wigand, M., Kaszuba, J. P., Carey, J. W., & Hollis, W. K. (2009). Geochemical effects of CO2 sequestration on fractured wellbore cement at the cement/caprock interface. *Chemical Geology,265*(1-2), 122-133. doi:10.1016/j.chemgeo.2009.04.008.

Yijin, Z. (2016). Study of Corrosion Mechanism of Sour Gas to Cement Stone in PUGUANG Gas Field. *International Journal of Petrochemical Science & Engineering,1*(1). doi:10.15406/ipcse.2016.01.00002.

VITA

Tri-Tris Bao Nguyen is a first generation Vietnamese-American born and raised in Woodland, California. In May of 2015, he graduated from the University of the Pacific in Stockton, California with a Bachelor of Science in Biochemistry. There, he worked as an undergraduate research assistant studying triplex forming oligonucleotides for potential application in human gene therapy. He is the first individual in his family to receive an advanced degree. In December of 2017, he earned a Master of Science in Petroleum Engineering from Missouri University of Science & Technology in Rolla, MO. During his time at Missouri S&T he worked to found the Drillbotics Design team, a student organization that designs and manufactures a fully automated drilling rig to create vertical wellbores in various formation types.